



Research paper

2-hydroxyisoquinoline-1,3(2*H*,4*H*)-diones (HIDs) as human immunodeficiency virus type 1 integrase inhibitors: Influence of the alkylcarboxamide substitution of position 4



Muriel Billamboz ^{a, b}, Virginie Suchaud ^{a, b}, Fabrice Bailly ^{a, b, *}, Cedric Lion ^{a, c}, Marie-Line Andréola ^d, Frauke Christ ^e, Zeger Debyser ^e, Philippe Cotelle ^{a, b}

^a Université Lille Nord de France, F-59000 Lille, France

^b Centre de Recherches Jean-Pierre Aubert UMR-S1172, Faculté des Sciences Pharmaceutiques et Biologiques, 3 rue du Professeur Laguesse, BP83, F-59006 Lille, France

^c UMR CNRS 8576, Unité de Glycobiologie Structurale et Fonctionnelle, F-59655 Villeneuve d'Ascq, France

^d Laboratoire MFP, UMR 5234 CNRS, Université Bordeaux Segalen, FR Transbiomed, 146 Rue Léo Saignat, F-33076 Bordeaux, France

^e Molecular Medicine, K.U. Leuven and IRC KULAK, Kapucijnenvoer 33, B-3000 Leuven, Flanders, Belgium

ARTICLE INFO

Article history:

Received 6 November 2015

Received in revised form

25 March 2016

Accepted 26 March 2016

Available online 28 March 2016

Keywords:

HIV-1 integrase

Two-metal binding pharmacophore

Antiretroviral

2-hydroxyisoquinoline-1,3(2*H*,4*H*)-diones

ABSTRACT

Herein, we report further insight into the biological activities displayed by the 2-hydroxyisoquinoline-1,3(2*H*,4*H*)-dione (HID) scaffold. Previous studies have evidenced the marked fruitful effect of substitution of this two-metal binding pharmacophore at position 4 by phenyl and benzyl carboxamido chains. Strong human immunodeficiency virus type 1 integrase (HIV-1 IN) inhibitors in the low nanomolar range with micromolar (even down to low nanomolar) anti-HIV activities were obtained. Keeping this essential 4-carboxamido function, we investigated the influence of the replacement of phenyl and benzyl groups by various alkyl chains. This study shows that the recurrent halogenobenzyl pharmacophore found in the INSTIs can be efficiently replaced by an n-alkyl group. With an optimal length of six carbons, we observed a biological profile and a high barrier to resistance equivalent to those of a previously reported hit compound bearing a 4-fluorobenzyl group.

© 2016 Elsevier Masson SAS. All rights reserved.

1. Introduction

Over the last two decades, intense efforts have been devoted to the development of HIV-1 integrase (IN) inhibitors and the pyrimidone scaffold was intensively investigated [1], leading to the release of Raltegravir (Fig. 1), the first HIV-1 IN inhibitor approved by the Food and Drug Administration (FDA) in 2007 [2], which opened up a new class of antiretrovirals agents [3,4]. It has become

a preferred first line agent as part of the highly active antiretroviral therapy (HAART) treatment guidelines since 2009 [5]. Indeed it has a favorable long-term efficacy and safety profile in integrase-inhibitor-naïve patients with triple-class resistant HIV in whom antiretroviral therapy is failing. However, after several years of clinical use, resistance to this integrase strand transfer inhibitor (INSTI) involving mutations at IN amino acids Y143, Q148, and N155 has quickly emerged [6–9]. Elvitegravir, the second FDA-approved INSTI, needs to be boosted by the pharmacoenhancer termed cobicistat and is prescribed as a potent once-daily single tablet also including two potent nucleos(t)ide reverse transcriptase inhibitors (NRTIs), emtricitabine and tenofovir [10–12]. Although this novel anti-HIV tablet could offer new perspective for patients failing existing antiviral regimes, cross resistance with raltegravir rules out any treatment option for patients failing on raltegravir therapy [13,14]. Dolutegravir, is a second generation integrase inhibitor that provides distinct advantages compared with first generation integrase inhibitors. Unlike raltegravir, dolutegravir in coformulation with abacavir and lamivudine can be given once daily for patients

Abbreviations: AZT, azidothymidine; CPE, cytopathic effect; CYP, cytochrome P450; FC, fold-change in EC₅₀ relative to wild-type strain of HIV-1; FDA, food and drug administration; LEDGF, lens epithelium-derived growth factor; HAART, highly active antiretroviral therapy; HID, 2-hydroxyisoquinoline-1,3(2*H*,4*H*)-dione; HIV-1, human immunodeficiency virus type 1; IN, integrase; INSTI, integrase strand transfer inhibitor; 3'-P, 3'-processing; PFV, prototype foamy virus; RT, reverse transcriptase; ST, strand transfer; TI, therapeutic index; TOA, time of addition.

* Corresponding author. Centre de Recherches Jean-Pierre Aubert UMR-S1172, Faculté des Sciences Pharmaceutiques et Biologiques, 3 rue du Professeur Laguesse, BP83, F-59006 Lille, France.

E-mail address: fabrice.bailly@univ-lille1.fr (F. Bailly).

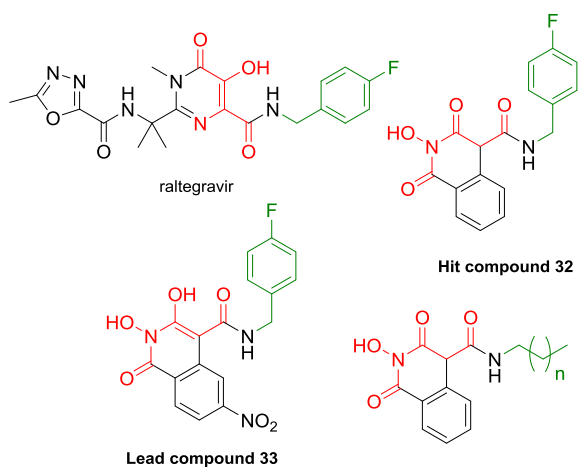


Fig. 1. Structures of the INSTI raltegravir, the hit compound **32**, the lead compound **33** and of herein studied *N*-alkyl carboxamides pointing out the key components of the HIV-1 IN inhibitory pharmacophore: the magnesium chelating moiety (red) and the hydrophobic halogenobenzyl or alkyl group (green). (For interpretation of the references to colour in this figure legend, the reader is referred to the web version of this article.)

who are antiretroviral treatment naïve without the requirement of a pharmacokinetic booster which minimizes the drug–drug interaction potential of dolutegravir [15–17]. Moreover, dolutegravir showed a more robust resistance profile than raltegravir and elvitegravir although some viruses containing E138K, G140S, or R148H mutations had lower susceptibility and may also diminish the likelihood of long-term clinical success [18,19]. All these INSTIs were shown to inhibit HIV-1 IN by chelating the two magnesium ions of the catalytic core through a triad of oxygen atoms [20,21]. Thus, in the current clinical context, integrase inhibitors should have a high genetic barrier to existing INSTIs to be novel serious candidates. For this purpose, alternative targets like the cellular cofactor lens epithelium-derived growth factor (LEDGF/p75) are promising targets [22,23] or continuous modulation of valuable scaffolds like naphthyridine is still relevant [24].

Following early pioneer studies on the 2-hydroxyisoquinoline-1,3-(2*H*,4*H*)-dione (HID) scaffold [25,26], we recently reported the interesting biological properties of some derivatives substituted at position 4 by carboxamide chains [27–29]. These compounds displayed strong IN inhibitory potencies comparable to that of the clinically used raltegravir. One hit compound **32** (Fig. 1) potently inhibited ST and 3' P IN catalytic activities while it kept activity against a panel of raltegravir-resistant HIV-1 variants and did not induce any resistance selection in cell culture [27]. A crystal structure of this compound bound to the wild-type prototype foamy virus (PFV) intasome revealed that the compact heterocyclic scaffold displaying all three Mg²⁺ chelating oxygen atoms from a single ring showed an overall binding mode similar to previous INSTIs [27]. Further substitution of this hit compound at position 7 by electron-withdrawing groups and particularly the nitro function led to the discovery of the lead compound **33** (Fig. 1) with low nanomolar anti-HIV potency [29].

Herein we elaborated and studied a novel series of 2-hydroxyisoquinoline-1,3-(2*H*,4*H*)-diones, in which we replaced the *p*-fluorobenzyl side chain by various alkyl chains. These synthetic modulations, aimed at generating more hydrophobic molecules, were performed in order to assess the influence of the nature of the side chain on the enzymatic inhibitory and antiviral properties within this scaffold. Owing to the nature of the hydrophobic pocket occupied by this substituent at the catalytic site (not only due to aromatic DNA bases pairs but also containing non-aromatic

hydrophobic aminoacid residues), we investigated whether the *N*-benzylated chain at position 4 of the HID scaffold could be replaced by alkyl chains that would occupy this cavity through pure van der Waals interactions.

2. Results and discussion

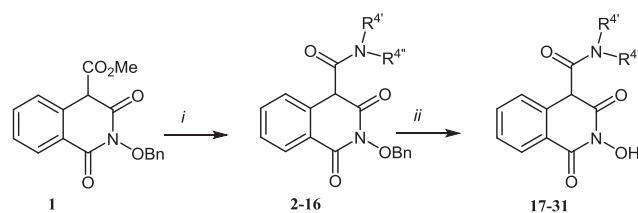
2.1. Chemistry

The target 2-hydroxyisoquinoline-1,3-(2*H*,4*H*)-diones were synthesized according to our previously reported method [28]. The key ester precursor **1**, methyl 2-(benzyloxy)-1,3-dioxo-1,2,3,4-tetrahydroisoquinoline-4-carboxylate was converted to carboxamides **2–16** by addition–elimination of various amines. Finally, the *O*-benzyl protecting group was removed by action of boron trichloride or hydrogenation at room temperature over 5% Pd/C (Scheme 1). A series of primary carboxamides with increasing linear alkyl chains (3–9 carbons, **17**, **19**, **23–27**) were synthesized (Table 1), together with representative secondary amides (compounds **20**, **21** and **31**). The influence of the ramification (compound **18**, R⁴ = isopropyl; compound **22**, R⁴ = *tert*butyl) of the alkyl chain and of the bulkiness (compound **28–30**, R⁴ = cyclopropyl, cyclopentyl, cyclohexyl) of the cycloalkyl chain was also briefly investigated.

2.2. Integrase and ribonuclease H inhibitory properties

Table 1 shows the biological properties of this series of *N*-alkyl-2-hydroxy-1,3-dioxoisoquinoline-4-carboxamides. As far as the compounds (**17**, **19**, **23–27**) with increasing linear chains are concerned, compounds **17** (R⁴ = propyl), **26** (R⁴ = octyl) and **27** (R⁴ = nonyl) displayed weakened HIV-1 IN inhibition when compared with our reference hit and lead compounds **32** and **33**, with IC₅₀ values of 1.82, 9.05 and 6.65 μM, respectively. Compounds **19**, **23**, and **25** (R⁴ = butyl, pentyl, and heptyl) inhibit HIV-1 IN in the submicromolar IC₅₀ range, with values from 0.65 μM to 0.86 μM. Compound **24** bearing an hexyl side-chain (IC₅₀ 0.085 μM) is the only representative in this series that displayed excellent integrase inhibitory activity in the same nanomolar range as lead **33** (IC₅₀ 0.010 μM). Fig. 2 shows the variation of the integrase inhibitory activity according to the length of the linear alkyl chain, clearly evidencing an optimal length of six carbons since compound **24** (R⁴ = hexyl, IC₅₀ = 0.085 μM) is 20- to 105-fold more active than compounds **17** (R⁴ = propyl, IC₅₀ = 1.82 μM), **26** (R⁴ = octyl, IC₅₀ = 9.05 μM) and **27** (R⁴ = nonyl, IC₅₀ = 6.65 μM) whereas there is only one-log difference with the close compounds **19** (R⁴ = butyl, IC₅₀ = 0.66 μM), **23** (R⁴ = pentyl, IC₅₀ = 0.65 μM) and **25** (R⁴ = heptyl, IC₅₀ = 0.86 μM).

The ramification of the propyl chain did not have a great impact on the integrase inhibition with close IC₅₀ values of 1.82 and 4.43 μM for the linear and ramified counterparts **17** and **18**,



Scheme 1. Synthesis of target compounds **17–31**. Reagents and conditions: (i) 2.0 eq. R₄NH₂, toluene, Dean Stark apparatus, reflux, 15 h (45–83%); (ii) BCl₃, 5.0 or 6.0 eq, CH₂Cl₂, 15 min, rt then H₂O, 5 min, rt (49–88%) or H₂, 5% Pd/C, EtOAc/MeOH, rt, 4 h (52–90%).

Table 1
Inhibition of HIV-1 in, antiviral activity, and cytotoxicity of substituted 2-hydroxyisoquinoline-1,3(2*H*,4*H*)-diones **17–34**, and raltegravir.

Keto form \rightleftharpoons Enol form

Comp.	R ⁷	R ^{4'}	R ^{4''}	IC ₅₀ (μM) Overall IN ^a	IC ₅₀ (μM) ST IN ^b	IC ₅₀ (μM) RNase H ^c	EC ₅₀ (μM) ^d	CC ₅₀ (μM) ^e	TI ^f
Raltegravir ²⁶				0.010	0.007		0.006	>8	>1333
17 (Keto) ^g	–H	–H	–(CH ₂) ₂ CH ₃	1.82	1.99		28.0	131	4.7
18 (Keto) ^g	–H	–H	–CH(CH ₃) ₂	4.43	5.05		30.2	162.5	5.4
19 (Keto) ^g	–H	–H	–(CH ₂) ₃ CH ₃	0.66	0.48	15.1	9.20	128	14
20 (Keto) ^g	–H	–CH ₃	–(CH ₂) ₃ CH ₃	8.66	8.70		>63.8	63.8	
21 (Keto) ^g	–H	–CH ₂ CH ₃	–CH ₂ CH ₃	123	206		>28	28	
22 (Keto) ^g	–H	–H	–C(CH ₃) ₃	4.45	4.46		>142	142	
23 (Keto) ^g	–H	–H	–(CH ₂) ₄ CH ₃	0.65	0.53		10.7	130	12.1
24 (Keto) ^g	–H	–H	–(CH ₂) ₅ CH ₃	0.085	0.195	5.35	2.70	57.7	21.2
25 (Keto) ^g	–H	–H	–(CH ₂) ₆ CH ₃	0.86	1.05	23.2	32.5	109.5	3.4
26 (Keto) ^g	–H	–H	–(CH ₂) ₇ CH ₃	9.05	9.13		28.0	98.5	3.5
27 (Keto) ^g	–H	–H	–(CH ₂) ₈ CH ₃	6.65	6.67		29.0	88.5	3.0
28 (Keto) ^g	–H	–H		2.13	4.00		42.7	>250	>6
29 (Keto) ^g	–H	–H		1.36	3.63		61.9	>250	>4
30 (Keto) ^g	–H	–H		0.7	3.36		80.2	>250	>3
31 (Keto) ^g	–H	–H		8.12	9.10		>120	120	
32 ²⁸ (Keto) ^g	–H	–H		0.056	0.099	0.36	2.34	202	86.3
33 ²⁹ (Enol) ^g	–NO ₂	–H		0.010	0.015		0.11	121	1100
34 ²⁹ (Enol) ^g	–NO ₂	–H	–(CH ₂) ₅ CH ₃	0.060	0.010		4.21	>250	>59

^{a,b,c} Concentration required to inhibit by 50% the *in vitro* overall integrase, strand transfer integrase and RNase H activities, respectively.

^d Effective concentration required to reduce HIV-1 induced cytopathic effect by 50% in MT-4 cells.

^e Cytotoxic concentration required to reduce by 50% MT-4 cell viability.

^f Therapeutic index defined by CC₅₀/EC₅₀ ratio.

^g Major tautomeric form present in DMSO solution.

respectively. On the contrary, the homologous compound **19** (R⁴ = butyl, IC₅₀ = 0.66 μM) did not retain its submicromolar inhibition upon ramification (compound **22**, R⁴ = *tert*-butyl, IC₅₀ = 4.45 μM). Cyclization of the linear alkyl chain did not strongly modify the antiintegrase activities of the C3 and C5 derivatives since compounds **17** (R⁴ = propyl, IC₅₀ = 1.82 μM) and **23** (R⁴ = pentyl, IC₅₀ = 0.65 μM) were as active as their respective

cyclic analogues **28** (R⁴ = cyclopropyl, IC₅₀ = 2.13 μM) and **29** (R⁴ = cyclopentyl, IC₅₀ = 1.36 μM). In contrast, the cyclic C6 compound **30** (R⁴ = cyclohexyl, IC₅₀ = 0.7 μM) was 8.2-fold less active than its acyclic counterpart **24** (R⁴ = hexyl, IC₅₀ = 0.085 μM). The extension of the cycle size was slightly favorable since the cyclic C6 compound **30** (R⁴ = cyclohexyl, IC₅₀ = 0.7 μM) was 3.0-fold more active than the cyclic C3 compound **28** (R⁴ = cyclopropyl, IC₅₀ = 2.13 μM) but integrase inhibition in the nanomolar range was not reached within this small cyclic series **28–30**. Secondary carboxamides **20**, **21** and **31** were revealed as modest integrase inhibitors with IC₅₀ values in the large micromolar range. The negative effect of a second alkyl group on the nitrogen atom of the carboxamide function is well pinpointed by comparison of the properties of the primary carboxamide **19** (IC₅₀ = 0.66 μM) and its methylated secondary derivative **20** (IC₅₀ = 8.66 μM). This evolution is corroborated by the study of our previous series of carboxamides [27,28]. We observed that replacing the amide proton by a methyl group provoked a strong decrease of the HIV-1 IN inhibition, which stressed the importance of an intramolecular hydrogen bond between the exocyclic amide hydrogen and the oxygen at position 3. Preliminary docking studies [28,29] subsequently followed by crystal structure of **32** in complex with the PFV IN intasome (PDB: 4IKF) [27] were in perfect accordance to support the hypothesis that this intramolecular hydrogen bond allows

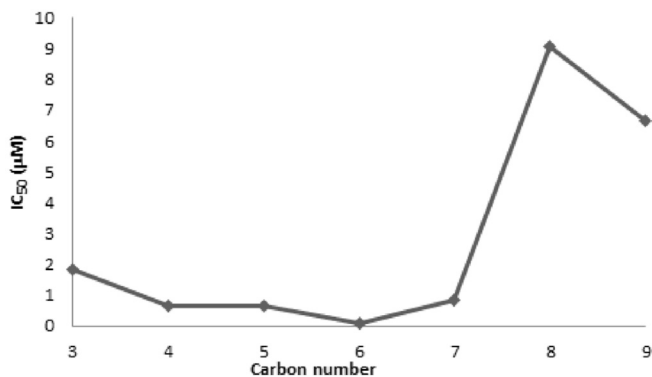


Fig. 2. Effect of the length of the linear alkyl side chain at position 4 on HIV-1 IN inhibitory activity of HIDs **17**, **19**, **23–27**.

convenient orientation of the side chain towards the desired hydrophobic pocket near the IN catalytic site. As a whole, the integrase inhibitory potencies of these alkyl carboxamides were weak with IC_{50} values in the large micromolar or submicromolar ranges. Replacing the phenyl and benzyl carboxamides at position 4 of the scaffold by alkyl carboxamides gave modest to good HIV-1 IN inhibitors. We previously obtained a reproducible low nanomolar antiintegrase potency within the phenyl and benzyl carboxamides series [27–29]. Herein, **24** reaches this level with an IC_{50} value ($IC_{50} = 0.085 \mu\text{M}$) close to those of our hit compound, **32** ($IC_{50} = 0.056 \mu\text{M}$) and the clinically used INSTI, raltegravir ($IC_{50} = 0.010 \mu\text{M}$). Crystal structure of **32** in complex with the PFV IN intasome (PDB:4IKF) showed that the extending *p*-fluorobenzyl group makes extensive van der Waals interactions with conserved residues P214 and Q215 (HIV equivalents P145, Q146), the invariant CA dinucleotide, and the guanosine 4 base from the nontransferred strand and stacks its aromatic ring against the 3' penultimate cytosine base [27]. The absence of an exocyclic aromatic ring making π – π stacking had to be compensated by optimized Van der Waals interactions. This was achieved with **24**: its optimal linear hexyl chain seems to interact as efficiently as **32** with HIV-1 catalytic core. Compounds' effects on HIV-1 ST activity was also examined (Table 1). Close values of the IN overall and ST inhibitions were observed for all the series, which may infer ST selectivity as it is well-known for the pioneer INSTI, raltegravir. However, the calculated ratio $IC_{50}(3'-P)/IC_{50}(ST)$ was measured at 6.0 for the hit compound **24** ($IC_{50}(3'-P) = 0.51 \mu\text{M}$), revealing a moderate ST

selectivity. This behavior was previously reported for similar isoquinoline-4-carboxamides [28]. We also tested some compounds against HIV-1 Reverse Transcriptase (RT) associated RNase H activity (Table 1) since this scaffold was originally developed for the design of dual inhibitors of HIV-1 IN and RT associated RNase H domain [25]. A micromolar IC_{50} value ($5.35 \mu\text{M}$) was obtained for compound **24** whereas compounds **19** and **25** were less inhibitory with IC_{50} values of 15.1 and 23.2 μM , respectively. In this series of alkylcarboxamides, the RNase H inhibition did not reach the submicromolar level obtained previously for some benzylcarboxamides [28].

2.3. Docking studies

The tendency observed for integrase inhibition was confirmed by *in silico* molecular docking studies on this series of HIDs bearing a linear alkyl side-chain **17**, **19**, **23–27** (Fig. 3 and see Supporting Information), applying our previously reported protocol [29].

In our previous work on compound **32** and other benzylated HIDs, we reported an optimized docking protocol based on the PDB:3S3M structure of the prototype foamy virus (PFV) co-crystallized with dolutegravir. We then confirmed the binding mode obtained with this procedure for **32** by experimental X-ray co-crystal structure in the PFV intasome [27–29]. These results evidenced that the dual chelation of the two magnesium co-factors within the catalytic site allows the N-benzylamido side chain to occupy a known hydrophobic pocket and interact with a cytosine

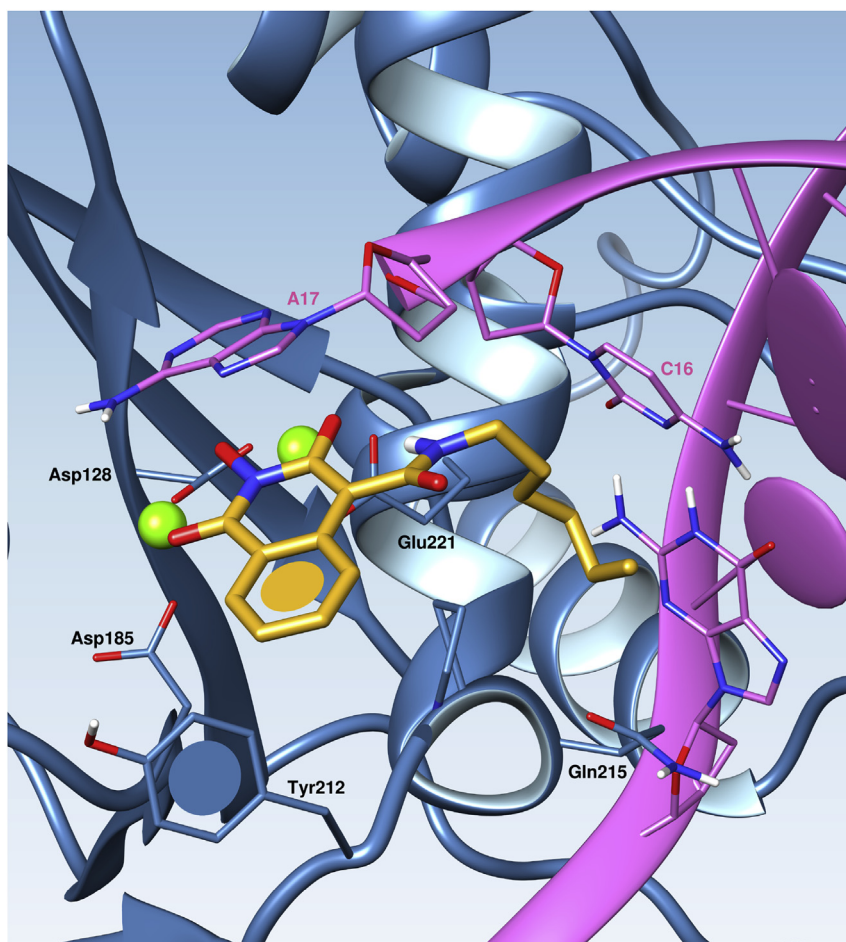


Fig. 3. Proposed binding mode of compound **24** as obtained by molecular docking in the PFV IN catalytic site (PDB:3S3M). Viral DNA is depicted in pink, PFV IN in blue, magnesium cations in green and the ligand in gold. (For interpretation of the references to colour in this figure legend, the reader is referred to the web version of this article.)

via π -stacking, in a similar way to dolutegravir. Although the real nature of π -stacking is still debated in the literature nowadays [30], the main energetic contribution to these interactions are Van Der Waals dispersion and electrostatics. Owing to the fact that the hydrophobic nature of the pocket created at the interface between integrase and the nucleic acid chain at the catalytic site is not only due to DNA bases but also to non-aromatic hydrophobic residues of the protein, it seemed natural to investigate whether or not replacing the benzylated side chain at position 4 by alkyl substituents could be beneficial.

As expected, the outcome of molecular docking for all compounds except for **17** was similar to that of our recently published 4-benzylcarboxamido derivatives. No satisfying docking pose could be obtained for propyl derivative **17**: the short 3-carbon side-chain is not long enough to occupy the hydrophobic pocket formed at the protein-DNA interface, natively occupied by the 3'-terminal base of viral DNA. Therefore compound **17** can efficiently chelate the two magnesium cofactors within the catalytic site, but there is no additional stabilizing interaction coming from the side-chain, which confirms the essential nature of this hydrophobic substituent. All the other compounds exhibited a clear docking pose similar to that obtained for our *p*-fluorobenzylated hit compounds [28,29]: the binding mode previously identified for **32** and **33** is retained with regard to chelation of both metallic cofactors by the pharmacophore and to the intramolecular H-bond within the ligand, stabilizing the side-chain in an ideal position for occupation of the hydrophobic pocket. Interestingly, the lack of π -stacking between the inhibitor and the penultimate cytosine of the DNA seems well compensated by hydrophobic interactions, the alkyl side-chain being ideally placed in the cavity, as observed in the different energetic terms of the obtained scores for the CHEMPLP function of the Gold docking suite, most notably the attractive hydrophobic–hydrophobic term (data not shown). This correlates with the fact that these alkyl derivatives maintain quite a good inhibitory activity on HIV-1 IN when compared to previously reported series that do not bear carboxamido groups in position 4 [26]. Because molecular docking is not quantitative and this docking protocol does not allow for flexibility of the DNA structure, it would seem hazardous to go further than a qualitative assessment here. However, this cavity being quite short in length, it appears that it cannot accommodate longer linear chains in their most stable conformation, thus requiring less favorable eclipsed conformations of the sp^3 -hybridized carbon atoms: the longer the hydrocarbon chain, the higher the internal torsion of the ligand. Additionally, in the identified poses, the termini of octyl and nonyl chains in compounds **26** and **27** is directly exposed to the aqueous medium and does not fit into the cavity. The fact that compound **24** exhibits the best activity in this series can be directly correlated to its optimal occupancy of the hydrophobic pocket (when compared to propyl **17**, butyl **19** and pentyl **23**) while minimizing conformational strain and water exposure of the side-chain (when compared to heptyl **25**, octyl **26** and nonyl **27**) (Fig. 2; see Supporting Information, superimposition of the best ligand docking poses).

2.4. Antiviral properties

To unambiguously attribute the antiviral activities of our HID compounds to a specific cell inhibition of HIV-1 IN, time-of-addition (TOA) experiments were first performed before doing the evaluation in a cell-based antiviral assay against HIV-1. Compound **24** was tested together with a set of known HIV replication inhibitors. The compounds were added at different time points after infection of MT-4 cells with HIV-1 IIIB, and p24 antigen production in the supernatants was measured at 30 h postinfection. The loss of activity was delayed to 4–5 h, 10–11 h,

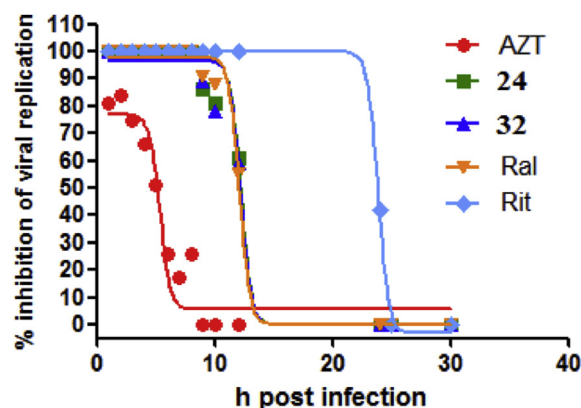


Fig. 4. Time-of-addition experiments. After infection of MT-4 cells with HIV-1 IIIB, inhibitors (50- and 100-fold EC_{50}) were added at indicated time points spanning from 1 to 25 h postinfection. Virus replication was determined by p24 antigen determination in the supernatant at 30 h postinfection. The comparative profiles of RT inhibitor, AZT, HDIs **24** and **32**, INSTI raltegravir (Ral) and protease inhibitor ritonavir (Rit) are presented.

25 h post-infection for RT inhibitor AZT, INSTI raltegravir and protease inhibitor ritonavir, respectively (Fig. 4). Compound **24** matched the profile observed for the INSTI raltegravir and our hit compound **32**, attesting for its cellular inhibition of HIV-1 integrase (Fig. 4).

Table 1 shows that HIV-1 IN inhibitions and antiviral activities can be reasonably correlated. Our new compounds were moderately active *in vitro* with EC_{50} values ranging from 9.2 to 51.8 μ M and four compounds (**20–22**, **31**) displayed limiting cellular cytotoxicity. Interestingly, compound **24** with the best antiintegrase activity of the series displayed also the lowest EC_{50} value of 2.70 μ M, roughly equal to that of hit compound **32** ($EC_{50} = 2.34 \mu$ M). An explanation for the lack of significant antiviral activities could be an unfavorable tautomeric equilibrium within this series of HDIs, whose major tautomeric form present in DMSO solution is the keto one (Table 1; see 1H and ^{13}C NMR spectra of compound **23** in Supporting Information). In contrast, we previously evidenced a good relationship between the enolization ability of HDIs and low submicromolar antiviral activities [29]. We found that the substitution by electron-withdrawing functions like cyano and, particularly nitro moieties led to the displacement of the keto-enol equilibrium towards enol compounds, with higher lipophilicities and improved anti-HIV activities [29]. Furthermore, careful comparison of the antiviral activities of the HDIs **24**, **32**, **33** and **34** (Table 1) evidences the cumulative positive effect of a *p*-fluorobenzyl group at position 4 and of a nitro function at position 7. Compound **34** bearing a hexyl chain at position 4 and a nitro function at position 7 was therefore synthesized. Even though its HIV-1 IN inhibitory activity was slightly improved when compared to its counterpart **24** ($IC_{50} = 0.060 \mu$ M vs. 0.085 μ M, respectively), the improvement upon introduction of this nitro substituent did not translate in terms of *in vivo* HIV-1 replication ($EC_{50} = 4.21 \mu$ M) as it did for *p*-

Table 2

Cross resistance of HDIs **24**, **32**, dolutegravir (Dol.) with INSTI raltegravir (Ral.). Fold-change (FC) in EC_{50} relative to wild-type strain of HIV-1.

Resistance	Virus strain	Ral. ²⁷	Dol.	24	32 ²⁷
Ral.	Q148H	9.0	n.d. ^a	1.0	1.0
	N155H	5.0	n.d. ^a	1.0	1.0
	G140S/Q148H	486	5.0	1.0	1.0

^a Not determined.

fluorobenzylated derivatives **32** ($EC_{50} = 2.34 \mu\text{M}$) and **33** ($EC_{50} = 0.11 \mu\text{M}$). Therefore, with this low nanomolar potency, derivative **33** remains the lead compound in this series.

Regarding the therapeutic index, the hit compound **24** (TI = 21.2; Table 1) was the best HID of the series. This encouraging result has to be improved to reach the level of compound **32** (TI = 86.3).

As mentioned before, the current primary objective for the development of novel marketable antiintegrase drugs is to discover compounds with minimal toxicity that retain good effectiveness against known resistant mutants [8,9,24]. This led us to test our hit compound **24** against the relevant Y143R, N155H mutants and also the double mutant, Q148H/G140S. Table 2 shows the fold changes in the EC_{50} values of compounds **24**, **32** and dolutegravir tested against raltegravir-resistant strains. Like the previous hit **32**, compound **24** retained completely its activity against N155H, Q148H mutants and the G140S/Q148H double mutant. For this double mutant, the HID compounds are even better than dolutegravir, which displayed a 5-fold change in EC_{50} .

2.5. Preliminary ADMETox evaluation of **24**

As reported for our previous lead compound **33**, we performed a preliminary ADMETox evaluation of **24** [29]. This hit compound displayed a good aqueous solubility of 160.3 μM (200.0 μM for **33**) and a partition coefficient, logD of 1.26 (1.24 for **33**). As for the compounds **32** and **33** [28,29], compound **24** presents a high human plasma protein binding (mean of 99.9% protein bound; mean of 93.2% recovery). However, regarding A-B permeability (Caco-2 cells, pH 6.5/7.4), a mean permeability coefficient P_{app} of 24.6×10^{-6} cm/s was determined at a 10 μM concentration while negligible values below 0.1 and 0.2×10^{-6} cm/s were obtained for **32** [28] and **33** [29], respectively. This represents a large advantage of **24** over **32** and **33**. This hit compound has satisfactory features for uptake after oral administration since a desired P_{app} value for a candidate drug should be $> 15.0 \times 10^{-6}$ cm/s. P-gp is an important transporter protein found in cells throughout the body, such as those lining the intestine and blood–brain barrier. It is believed to play an important role in defining the extent of distribution of drug molecules and limiting their oral and brain exposures. Up to a concentration of 100.0 μM , compound **24** like **32** and **33**, inhibited the P-gp efflux at a minor extent (Table 3) while the reference compound, verapamil, reduced by 50% this efflux at a concentration of 8.0 μM . The cytochrome P450 (CYP) is a large superfamily of enzymes involved in drug metabolism via oxidation of organic substances. Changes in the activity or expression levels of CYPs are the major source of adverse effects of drugs. As shown in Table 3, **24** like **32** at a concentration of 10 μM only faintly inhibited up to 25.0% the different CYPs tested (CYP1A2, CYP2C9,

CYP2C19 and CYP2D6). The largest inhibition (42.0%) was observed with CYP3A4, but it did not reach the marked unfavorable effect of **33** (100%). In addition, an extended study on the toxicity of this compound was performed (Table 4). The effects on cell number, intracellular free calcium, nuclear size, membrane permeability, and mitochondrial potential were measured. Compound **24** like **32** and **33** did not display any severe toxicity in these tests, even at a concentration of 100 μM . In contrast, the reference compound, cerivastatin, displayed submicromolar IC_{50} values for each test. Finally compound **24** was tested in a hERG (human Ether-a-go-go-Related Gene potassium channel 1; Table 5) inhibition assay. Inhibition of this voltage gated potassium ion channel, a transmembrane protein encoded by the hERG gene, is known to be undesirable due to the possibility of QT prolongation, which can lead to fatal cardiac arrhythmia. Compound **24** like **32** and **33** did not significantly inhibited the tail current with 5.8, 12.2 and 19.4% inhibitions at the concentrations of 0.1 μM , 1.0 μM and 10 μM , respectively. In the same conditions, the control compound E-4031 induced hERG-mediated cardiac toxicity with an IC_{50} value of 24 nM.

3. Conclusion

Herein, we investigated the antiintegrase and antiviral properties of a novel series of HIDs substituted at position 4 by various alkylcarboxamides. With the objective to replace the recurrent halobenzyl pharmacophore by a simple alkyl group, we found one hit compound **24** displaying integrase inhibition in the low nanomolar range. Its EC_{50} value on HIV-1 replication, is equivalent to that of compound **32**. This study evidenced an optimal length of six carbons for the alkyl side chain that can be correlated with the optimal fitting within the hydrophobic pocket created by displacement of the 3'-adenosine (A17). The importance of a primary carboxamido side function to allow for an intramolecular hydrogen bond between the amide proton and the carbonyl oxygen at position 3 was confirmed. On the whole, the preliminary ADMETox assessment of compound **24** evidenced a pharmacokinetic profile similar to that of our previous hit **32**. High plasma protein binding is still certainly responsible for the lack of strong nanomolar antiviral activity. But, without any severe toxicity, compound **24** is the first HID displaying a largely positive mean permeability coefficient P_{app} of 24.6×10^{-6} cm/s with satisfactory features for uptake after oral administration. Moreover, in contrast to dolutegravir, compound **24** retained completely its antiviral activity against the relevant mutants Q148H, N155H and the double mutant G140S/Q148H. To our knowledge, these HID compounds are the unique HIV-1 IN inhibitors able to display such properties against resistant IN mutants. The advantageous permeability coefficient of compound **24** and its high barrier to resistance will

Table 3

Inhibition of different members of the cytochrome P450 (CYP450) mixed-function oxidase system and of P-gp efflux by HIDs **24**, **32**, **33** and reference compounds.

Comp.	CYP1A2	CYP2C9	CYP2C19	CYP2D6	CYP3A4	P-gp inhibition (MDR1-MDCKII)		
24	12.7 ^a	25.3 ^a	9.3 ^a	24.6	42.0 ^a	-5.5 ^c	2.0 ^d	5.3 ^e
32 ²⁷	5.2 ^a	6.4 ^a	18.0 ^a	6.6	35.9 ^a	-5.4 ^c	-4.0 ^d	-3.7 ^e
33 ²⁹	1.4 ^a	76.5 ^a	11.4 ^a	Nd ^b	106 ^a	-5.1 ^c	-3.2 ^d	7.6 ^e
Furaflyline	1.4 ^f	Nd	Nd	Nd	Nd			
Sulphaphenazole	Nd	0.18 ^f	Nd	Nd	Nd			
Tranilcypromine	Nd	Nd	3.1 ^f	Nd	Nd			
Quinidine	Nd	Nd	Nd	0.017 ^f	Nd			
Ketoconazole	Nd	Nd	Nd	Nd	0.28 ^f			

^{c,d,e} P-gp inhibition at 1.0 μM , 30.0 μM and 100.0 μM .

^f IC_{50} values in μM .

^a Percentage inhibition of control values at a 10.0 μM dose.

^b Not determined.

Table 4
Detailed analysis of in vitro toxicity of HIDs **24**, **32**, **33** and cerivastatin.

Assay	Comp.	1.0 μM	30.0 μM	100.0 μM	IC ₅₀ (μM) ^f
Cytotoxicity (cell number) ^a	24	−10.0	4.9	25.3	Nd
	32 ²⁷	−22.8	25.7	16.0	Nd
	33 ²⁹	−20.1	12.6	−7.4	Nd
	Cerivastatin	Nd ^g	Nd	Nd	0.96
Intracellular free calcium ^b	24	−1.5	5.8	32.3	Nd
	32 ²⁷	−1.7	9.6	29.9	Nd
	33 ²⁹	−1.3	18.8	18.3	Nd
	Cerivastatin	Nd	Nd	Nd	0.34
Nuclear size ^c	24	−7.0	12.1	26.8	Nd
	32 ²⁷	−1.0	13.1	18.7	Nd
	33 ²⁹	2.0	23.8	22.1	Nd
	Cerivastatin	Nd	Nd	Nd	0.13
Membrane permeability ^d	24	0.1	7.0	23.6	Nd
	32 ²⁷	−0.5	20.3	41.2	Nd
	33 ²⁹	0	23.9	6.7	Nd
	Cerivastatin	Nd	Nd	Nd	0.80
Mitochondrial membrane potential ^e	24	5.7	5.1	33.9	Nd
	32 ²⁷	11.8	−21.2	6.3	Nd
	33 ²⁹	8.4	−23.8	22.4	Nd
	Cerivastatin	Nd	Nd	Nd	0.60

^a Percentage reduction relative to untreated control.^b Percentage increase relative to untreated control.^c Percentage reduction relative to untreated control.^d Percentage increase relative to untreated control.^e Percentage reduction relative to untreated control.^f Concentration required to inhibit a–e.^g Not determined.**Table 5**
Analysis of cardiac toxicity of HIDs **24**, **32**, **33** and the reference compound E-4031 (hERG automated patch-clamp).

Comp.	0.1 μM	1.0 μM	10.0 μM	IC ₅₀ (μM)
24	5.8 ^a	12.2	19.4	Nd
32 ²⁷	3.4	10.6	13.3	Nd
33 ²⁹	2.6	5.1	3.9	Nd
E-4031	Nd ^b	Nd	Nd	0.024

^a Percentage inhibition of tail current.^b Not determined.

encourage us to further pharmacomodulate this scaffold and reach antiviral activities in the nanomolar range. In order to overcome high plasma protein binding and improve the biological properties within this series, alkyl side chains containing heteroatoms may be inserted at position 4 of compound **24** or on its unsubstituted aromatic benzenic ring.

4. Experimental section

4.1. Chemistry

4.1.1. General details

All reagents and solvents were purchased from Aldrich-Chimie (Saint-Quentin-Fallavier, France) of ACS reagent grade and were used as provided. Thin layer chromatography analyses were performed on plastic sheets precoated with silica gel 60F254 (Merck). SiO₂, 40–63 mesh (Merck) or 30 μm HP-Silprepacked SNAP columns (Biotage) were used for flash column chromatography. NMR spectra were obtained on an AC 300 Bruker spectrometer in the appropriate solvent with TMS as internal reference. Chemical shifts are reported in δ units (ppm) and are assigned as singlets (s), doublets (d), doublets of doublets (dd), triplets (t), quartets (q), quintets (quin), sextuplets (sext), multiplets (m), and broad signals (br) ... Melting points were obtained on a Reichert Thermopan melting point apparatus, equipped with a microscope and are

uncorrected. Mass spectra (ElectroSpray Ionization, ESI) were recorded on a Micromass Quattro II spectrometer. HRMS measurements were made on an Apex Qe 9.4 T Bruker Daltonics spectrometer. Analytes dissolved in methanol (3 mM solutions) were diluted with a water/methanol/formic acid solution (50/50/0.1, % v/v) to afford 3 μM solutions and infused into the mass spectrometer nano ESI source in positive mode at a rate of 1 $\mu\text{L}/\text{min}$. The purity of the tested compounds was established by combustion analysis, confirming a purity $\geq 95\%$. Elemental analyses (C, H, N) were performed by CNRS laboratories (Vernaison, France); the analytical results were within $\pm 0.4\%$ of the theoretical values.

4.1.2. Synthesis of the carboxamides **2–16**

4.1.2.1. N-Propyl-2-benzyloxy-1,3-dioxo-1,2,3,4-tetrahydroisoquinoline-4-carboxamide (2). Ester **1** (0.32 g, 1.0 mmol) and propylamine (0.12 g, 2.0 mmol) were dissolved in toluene (100 mL). The mixture was refluxed for 15 h using a Dean Stark apparatus. After cooling, the solution was concentrated *in vacuo*. The residue was dissolved in EtOAc. The organic layer was washed with 2.0 M HCl and dried over Na₂SO₄. After concentration *in vacuo*, the residue was triturated in ether and the precipitate was filtered and dried at room temperature giving **2** as a white solid (80%); mp 166 °C; 100% keto form; ¹H NMR (300 MHz, DMSO-*d*₆): δ = 0.86 (t, 3 H, CH₃, ³J = 7.3 Hz), 1.45 (sext, 2 H, CH₂, ³J = 7.1 Hz), 3.06 (q, 2 H, NH-CH₂, ³J = 6.3 Hz), 4.98 (d, 1 H, OCH₂, ²J = 9.8 Hz), 5.03 (d, 1 H, OCH₂, ²J = 9.8 Hz), 5.12 (s, 1 H, CH), 7.38–7.45 (m, 4 H, H_{Ar}), 8.10 (d, 1 H, H_{Ar}, ³J = 7.8 Hz), 8.80 (t, 1 H, NH, ³J = 5.4 Hz); ¹³C NMR (75 MHz, DMSO-*d*₆): δ = 11.3 (CH₃), 22.2 (CH₂), 40.9 (CH₂), 55.8 (CH), 77.4 (OCH₂), 125.3 (C_{IV}), 126.6 (CH), 128.1 (CH), 128.3 (CH), 128.4 (2 CH), 128.9 (CH), 129.4 (2 CH), 134.2 (CH), 134.5 (C_{IV}), 133.9 (C_{IV}), 161.1 (CO), 164.6 (CO), 167.0 (CO); ESI-MS: *m/z* = 353 (M + H)⁺.

4.1.2.2. N-Isopropyl-2-benzyloxy-1,3-dioxo-1,2,3,4-tetrahydroisoquinoline-4-carboxamide (3). White solid (74%); mp 158 °C; 100% keto form; ¹H NMR (300 MHz, DMSO-*d*₆): δ = 1.07 (d, 3 H, CH₃, ³J = 6.4 Hz), 1.14 (d, 3 H, CH₃, ³J = 6.4 Hz), 3.76 (sext, 1 H,

CH, $^3J = 6.6$ Hz), 4.99 (d, 1 H, OCH₂, $^2J = 9.6$ Hz), 5.04 (d, 1 H, OCH₂, $^2J = 9.6$ Hz), 5.08 (s, 1 H, CH), 7.42–7.45 (m, 4 H, H_{Ar}), 7.57–7.60 (m, 3 H, H_{Ar}), 7.74 (t, 1 H, H_{Ar}, $^3J = 7.2$ Hz), 8.10 (d, 1 H, H₈, $^3J = 7.7$ Hz), 8.74 (d_{app}, 1 H, NH, $^3J = 7.4$ Hz); ^{13}C NMR (75 MHz, DMSO-*d*₆): $\delta = 22.0$ (2 CH₃), 41.3 (CH), 55.7 (CH), 77.3 (OCH₂), 125.2 (CH), 128.0 (CH), 128.3 (3 CH), 128.8 (CH), 129.4 (2 CH), 134.1 (CH), 134.4 (C_{IV}), 134.9 (C_{IV}), 161.1 (CO), 164.5 (CO), 165.0 (CO); ESI-MS: *m/z* = 353 (M + H)⁺.

4.1.2.3. *N*-Butyl-2-benzyloxy-1,3-dioxo-1,2,3,4-tetrahydroisoquinoline-4-carboxamide (**4**). White solid (83%); mp 166 °C; 100% keto form; ^1H NMR (300 MHz, CDCl₃): $\delta = 0.85$ (t, 3 H, CH₃, $^3J = 7.0$ Hz), 1.12–1.40 (m, 4 H, 2 CH₂), 3.28 (q, 2 H, NH–CH₂, $^3J = 6.9$ Hz), 4.80 (s, 1 H, CH), 5.14 (s, 2 H, OCH₂), 6.47 (t, 1 H, NH, $^3J = 7.0$ Hz), 7.40 (d, 1 H, H_{Ar}, $^3J = 7.7$ Hz), 7.52 (t, 1 H, H_{Ar}, $^3J = 7.6$ Hz), 7.69 (t, 1 H, H_{Ar}, $^3J = 7.4$ Hz), 8.07 (d, 1 H, H₈, $^3J = 6.8$ Hz); ^{13}C NMR (75 MHz, CDCl₃): $\delta = 13.7$ (CH₃), 20.0 (CH₂), 31.3 (CH₂), 40.3 (CH₂), 55.7 (CH), 78.5 (OCH₂), 125.3 (C_{IV}), 128.1 (CH), 128.5 (2 CH), 128.7 (CH), 129.0 (CH), 129.2 (CH), 130.0 (2 CH), 133.0 (C_{IV}), 133.8 (C_{IV}), 134.0 (CH), 161.1 (CO), 164.6 (CO), 165.1 (CO); ESI-MS: *m/z* = 367 (M + H)⁺.

4.1.2.4. *N*-Butyl-*N*-methyl-2-benzyloxy-1,3-dioxo-1,2,3,4-tetrahydroisoquinoline-4-carboxamide (**5**). White solid (69%); mp 117–120 °C; 100% keto form; ^1H NMR (300 MHz, CDCl₃): $\delta = 0.83$ (t, 3 H, CH₃, $^3J = 8.4$ Hz), 1.20–1.59 (m, 4 H, 2 CH₂), 2.88 (s, 3 H, NH–CH₃), 3.07 (s, 3 H, NH–CH₃), 3.30 (t, 2 H, NH–CH₂, $^3J = 6.7$ Hz), 3.56 (t, 2 H, NH–CH₂, $^3J = 6.7$ Hz), 4.99 (s, 1 H, CH), 5.23 (s, 1 H, CH), 7.06 (m, 1 H, H_{Ar}), 7.23–7.25 (m, 3 H, H_{Ar}), 7.36–7.47 (m, 4 H, H_{Ar}), 8.10 (d, 1 H, H₈, $^3J = 7.2$ Hz); ^{13}C NMR (75 MHz, CDCl₃): $\delta = 13.8$ (CH₃), 19.9 (CH₂), 20.0 (CH₂), 29.0 (CH₂), 30.9 (CH₂), 34.6 (NHCH₃), 36.5 (NHCH₃), 48.6 (NHCH₂), 51.0 (NHCH₂), 51.7 (CH), 52.5 (CH), 78.4 (OCH₂), 125.9 (C_{IV}), 126.1 (C_{IV}), 126.4 (CH), 128.4 (2 CH), 128.6 (CH), 129.0 (CH), 129.3 (CH), 129.9 (2 CH), 133.9 (C_{IV}), 134.2 (CH), 161.1 (CO), 164.2 (CO), 165.9 (CO); ESI-MS: *m/z* = 381 (M + H)⁺.

4.1.2.5. *N,N*-Diethyl-2-benzyloxy-1,3-dioxo-1,2,3,4-tetrahydroisoquinoline-4-carboxamide (**6**). White solid (67%); mp 114 °C; 100% keto form; ^1H NMR (300 MHz, DMSO-*d*₆): $\delta = 1.11$ (t, 3 H, CH₃, $^3J = 6.7$ Hz), 1.29 (t, 3 H, CH₃, $^3J = 6.5$ Hz), 3.24–3.43 (m, 2 H, NH–CH₂), 3.61–3.76 (m, 2 H, NH–CH₂), 5.00 (s, 2 H, OCH₂), 5.80 (s, 1 H, CH), 6.50 (s, 1 H, NH), 7.28 (d, 1 H, H_{Ar}, $^3J = 7.7$ Hz), 7.30–7.40 (m, 3 H, H_{Ar}), 7.56–7.61 (m, 3 H, H_{Ar}), 7.74 (t, 1 H, H_{Ar}, $^3J = 7.2$ Hz), 8.11 (d, 1 H, H₈, $^3J = 7.6$ Hz); ^{13}C NMR (75 MHz, DMSO-*d*₆): $\delta = 12.7$ (CH₃), 14.7 (CH₃), 40.5 (CH₂), 42.8 (CH₂), 51.1 (CH), 77.4 (OCH₂), 125.5 (C_{IV}), 126.6 (CH), 128.1 (CH), 128.2 (CH), 128.4 (2 CH), 128.9 (CH), 129.4 (2 CH), 134.3 (CH), 135.3 (2 C_{IV}), 160.9 (CO), 164.5 (CO), 165.7 (CO); ESI-MS: *m/z* = 367 (M + H)⁺.

4.1.2.6. *N*-Tert-butyl-2-benzyloxy-1,3-dioxo-1,2,3,4-tetrahydroisoquinoline-4-carboxamide (**7**). Beige solid (70%); mp 143 °C; 100% keto form; ^1H NMR (300 MHz, DMSO-*d*₆): $\delta = 1.31$ (s, 9 H, 3 CH₃), 5.04 (d, 1 H, OCH₂, $^2J = 9.3$ Hz), 5.08 (d, 1 H, OCH₂, $^2J = 9.3$ Hz), 5.19 (s, 1 H, CH), 7.48 (m, 3 H, H_{Ar}), 7.51 (d, 1 H, H_{Ar}, $^3J = 7.7$ Hz), 7.60–7.65 (m, 3 H, H_{Ar}), 7.80 (t, 1 H, H_{Ar}, $^3J = 7.7$ Hz), 8.15 (d, 1 H, H₈, $^3J = 7.7$ Hz), 8.55 (s, 1 H, NH); ^{13}C NMR (75 MHz, DMSO-*d*₆): $\delta = 28.1$ (3 CH₃), 50.9 (C_{IV}), 56.2 (CH), 77.3 (OCH₂), 125.2 (C_{IV}), 126.4 (CH), 128.0 (CH), 128.3 (2 CH), 128.8 (CH), 129.3 (2 CH), 134.0 (CH), 134.5 (C_{IV}), 135.1 (C_{IV}), 161.1 (CO), 164.6 (CO), 165.2 (CO); ESI-MS: *m/z* = 367 (M + H)⁺.

4.1.2.7. *N*-Pentyl-2-benzyloxy-1,3-dioxo-1,2,3,4-tetrahydroisoquinoline-4-carboxamide (**8**). White solid (45%); mp 134 °C; 100% keto form; ^1H NMR (300 MHz, CDCl₃): $\delta = 0.90$ (t, 3 H, CH₃, $^3J = 6.4$ Hz), 1.32–1.65 (m, 6 H, 3 CH₂), 3.25 (q, 2 H, NH–CH₂,

$^3J = 7.0$ Hz), 4.79 (s, 1 H, CH), 5.11 (d, 1 H, OCH₂, $^2J = 9.0$ Hz), 5.15 (d, 1 H, OCH₂, $^2J = 9.0$ Hz), 6.50 (s, 1 H, NH), 7.34–7.66 (m, 8 H, H_{Ar}), 8.24 (d, 1 H, H₈, $^3J = 7.3$ Hz); ^{13}C NMR (75 MHz, CDCl₃): $\delta = 13.9$ (CH₃), 22.2 (CH₂), 28.9 (2 CH₂), 40.5 (CH₂), 55.7 (CH), 78.5 (OCH₂), 125.3 (C_{IV}), 127.8 (CH), 128.5 (2 CH), 128.6 (CH), 128.9 (CH), 129.1 (CH), 129.9 (2 CH), 133.1 (C_{IV}), 133.8 (C_{IV}), 134.0 (CH), 161.1 (CO), 164.9 (CO), 165.0 (CO); ESI-MS: *m/z* = 381 (M + H)⁺.

4.1.2.8. *N*-Hexyl-2-benzyloxy-1,3-dioxo-1,2,3,4-tetrahydroisoquinoline-4-carboxamide (**9**). White solid (83%); mp 139–140 °C; 100% keto form; ^1H NMR (300 MHz, CDCl₃): $\delta = 0.88$ (t, 3 H, CH₃, $^3J = 7.0$ Hz), 1.29 (m, 6 H, CH₂), 1.51 (quin, 2 H, CH₂, $^3J = 7.0$ Hz), 3.25 (t, 2 H, CH₂, $^3J = 7.0$ Hz), 4.80 (s, 1 H, CH), 5.12 (d, 1 H, OCH₂, $^2J = 9.2$ Hz), 5.16 (d, 1 H, OCH₂, $^2J = 9.2$ Hz), 6.51 (t, 1 H, NH, $^3J = 6.0$ Hz), 7.28 (dd, 1 H, H₅, $^3J = 8.0$ Hz, $^4J = 1.5$ Hz), 7.30–7.40 (m, 3 H, H_{Ar}), 7.51–7.68 (m, 4 H, H_{Ar}), 8.23 (dd, 1 H, H₈, $^3J = 8.0$ Hz, $^4J = 1.5$ Hz); ^{13}C NMR (75 MHz, CDCl₃): $\delta = 14.0$ (CH₃), 22.5 (CH₂), 26.4 (CH₂), 29.2 (CH₂), 31.4 (CH₂), 40.6 (CH₂), 55.5 (CH), 78.6 (OCH₂), 125.2 (C_{IV}), 128.5 (2 CH), 128.6 (CH), 128.8 (CH), 129.0 (CH), 129.2 (CH), 130.0 (2 CH), 132.7 (C_{IV}), 133.7 (C_{IV}), 133.9 (CH), 160.5 (CO), 164.0 (CO), 165.1 (CO); ESI-MS: *m/z* = 395 (M + H)⁺.

4.1.2.9. *N*-Heptyl-2-benzyloxy-1,3-dioxo-1,2,3,4-tetrahydroisoquinoline-4-carboxamide (**10**). White solid (48%); mp 131–134 °C; 100% keto form; ^1H NMR (300 MHz, CDCl₃): $\delta = 0.80$ (t, 3 H, CH₃, $^3J = 7.0$ Hz), 1.19–1.21 (m, 8 H, 4 CH₂), 1.43–1.45 (m, 2 H, CH₂), 3.14 (q, 2 H, NH–CH₂, $^3J = 7.1$ Hz), 4.71 (s, 1 H, CH), 5.05 (m, 2 H, OCH₂), 6.40 (m, 1 H, NH), 7.19 (d, 1 H, H_{Ar}, $^3J = 7.2$ Hz), 7.26–7.30 (m, 3 H, H_{Ar}), 7.44–7.56 (m, 4 H, H_{Ar}), 8.16 (d, 1 H, H₈, $^3J = 8.3$ Hz); ^{13}C NMR (75 MHz, CDCl₃): $\delta = 14.1$ (CH₃), 22.6 (CH₂), 26.8 (CH₂), 28.9 (CH₂), 29.3 (CH₂), 31.7 (CH₂), 40.5 (CH₂), 55.7 (CH), 78.5 (OCH₂), 125.3 (C_{IV}), 127.8 (CH), 128.5 (3 CH), 129.0 (CH), 129.2 (CH), 129.9 (2 CH), 133.2 (C_{IV}), 133.8 (C_{IV}), 134.0 (CH), 161.2 (CO), 165.0 (CO), 165.1 (CO); ESI-MS: *m/z* = 409 (M + H)⁺.

4.1.2.10. *N*-Octyl-2-benzyloxy-1,3-dioxo-1,2,3,4-tetrahydroisoquinoline-4-carboxamide (**11**). White solid (49%); mp 137–139 °C; 100% keto form; ^1H NMR (300 MHz, CDCl₃): $\delta = 0.80$ (t, 3 H, CH₃, $^3J = 7.3$ Hz), 1.18–1.22 (m, 10 H, 5 CH₂), 1.43–1.45 (m, 2 H, CH₂), 3.18 (q, 2 H, NH–CH₂, $^3J = 7.5$ Hz), 4.71 (s, 1 H, CH), 5.07 (m, 2 H, OCH₂), 6.37 (m, 1 H, NH), 7.20 (d, 1 H, H_{Ar}, $^3J = 8.0$ Hz), 7.31–7.33 (m, 3 H, H_{Ar}), 7.44–7.59 (m, 4 H, H_{Ar}), 8.16 (d, 1 H, H₈, $^3J = 7.7$ Hz); ^{13}C NMR (75 MHz, CDCl₃): $\delta = 14.1$ (CH₃), 22.6 (CH₂), 26.8 (CH₂), 29.2 (3 CH₂), 31.8 (CH₂), 40.5 (CH₂), 55.7 (CH), 78.5 (OCH₂), 125.3 (C_{IV}), 127.8 (CH), 128.5 (3 CH), 128.9 (CH), 129.2 (CH), 129.9 (2 CH), 133.2 (C_{IV}), 133.8 (C_{IV}), 134.0 (CH), 161.1 (CO), 165.0 (CO), 165.1 (CO); ESI-MS: *m/z* = 423 (M + H)⁺.

4.1.2.11. *N*-Nonyl-2-benzyloxy-1,3-dioxo-1,2,3,4-tetrahydroisoquinoline-4-carboxamide (**12**). White solid (65%); mp 146 °C; 100% keto form; ^1H NMR (300 MHz, CDCl₃): $\delta = 0.89$ (t, 3 H, CH₃, $^3J = 7.0$ Hz), 1.28–1.60 (m, 14 H, 7 CH₂), 3.28 (q, 2 H, NH–CH₂, $^3J = 6.0$ Hz), 4.78 (s, 1 H, CH), 5.14 (m, 2 H, OCH₂), 6.43 (m, 1 H, NH), 7.30–7.68 (m, 8 H, H_{Ar}), 8.25 (d, 1 H, H₈, $^3J = 7.6$ Hz); ^{13}C NMR (75 MHz, CDCl₃): $\delta = 14.1$ (CH₃), 22.6 (CH₂), 26.8 (2 CH₂), 29.2 (3 CH₂), 29.5 (CH₂), 31.8 (CH₂), 40.5 (CH₂), 55.7 (CH), 78.5 (OCH₂), 125.3 (C_{IV}), 127.9 (CH), 128.5 (2 CH), 128.6 (CH), 128.9 (CH), 129.1 (CH), 129.9 (2 CH), 133.1 (C_{IV}), 133.8 (C_{IV}), 134.0 (CH), 161.1 (CO), 164.8 (CO), 165.0 (CO); ESI-MS: *m/z* = 437 (M + H)⁺.

4.1.2.12. *N*-Cyclopropyl-2-benzyloxy-1,3-dioxo-1,2,3,4-tetrahydroisoquinoline-4-carboxamide (**13**). White solid (71%); mp 183 °C; 100% keto form; ^1H NMR (300 MHz, DMSO-*d*₆): $\delta = 0.37$ –0.52 (m, 2 H, 2 CH), 0.62–0.75 (m, 2 H, 2 CH), 2.63–2.72 (m, 1 H, CH), 5.00 (d, 1 H, OCH₂, $^2J = 10.0$ Hz), 5.04 (d, 1 H, OCH₂,

$^2J = 10.0$ Hz), 5.00 (s, 1 H, CH), 7.34–7.50 (m, 4 H, H_{Ar}), 7.51–7.65 (m, 3 H, H_{Ar}), 7.74 (t, 1 H, H_{Ar} , $^3J = 7.4$ Hz), 8.10 (d, 1 H, H_8 , $^3J = 7.4$ Hz), 8.90 (d, 1 H, NH, $^3J = 3.1$ Hz); ^{13}C NMR (75 MHz, DMSO- d_6): $\delta = 6.6$ (2 CH_2), 23.7 (CH_2), 56.4 (CH), 55.6 (CH), 78.2 (OCH_2), 120.0 (C_{IV}), 126.1 (C_{IV}), 127.4 (CH), 128.9 (CH), 129.1 (2 CH), 129.2 (2 CH), 129.7 (CH), 130.2 (2 CH), 135.0 (CH), 135.5 (C_{IV}), 161.9 (CO), 165.2 (CO), 167.8 (CO); ESI-MS: $m/z = 351$ (M + H) $^+$.

4.1.2.13. N-Cyclopentyl-2-benzyloxy-1,3-dioxo-1,2,3,4-tetrahydroisoquinoline-4-carboxamide (14). White solid (77%); mp 188 °C; 100% keto form; 1H NMR (300 MHz, DMSO- d_6): $\delta = 1.40$ – 1.90 (m, 8 H, 4 CH_2), 3.95 (sext, 1 H, CH, $^3J = 6.3$ Hz), 4.99 (d, 1 H, OCH_2 , $^2J = 9.6$ Hz), 5.04 (d, 1 H, OCH_2 , $^2J = 9.6$ Hz), 5.10 (s, 1 H, CH), 7.40–7.43 (m, 4 H, H_{Ar}), 7.55–7.59 (m, 3 H, H_{Ar}), 7.74 (t, 1 H, H_{Ar} , $^3J = 7.6$ Hz), 8.09 (d, 1 H, H_8 , $^3J = 7.9$ Hz), 8.79 (d_{app} , 1 H, NH, $^3J = 7.3$ Hz); ^{13}C NMR (75 MHz, DMSO- d_6): $\delta = 23.4$ (CH_2), 23.5 (CH_2), 32.1 (CH_2), 32.2 (CH_2), 50.9 (CH), 55.6 (CH), 77.3 (OCH_2), 125.2 (C_{IV}), 126.4 (CH), 128.0 (CH), 128.2 (CH), 128.3 (2 CH), 128.8 (CH), 129.3 (2 CH), 134.1 (CH), 134.4 (C_{IV}), 134.9 (C_{IV}), 161.0 (CO), 164.5 (CO), 165.3 (CO); ESI-MS: $m/z = 379$ (M + H) $^+$.

4.1.2.14. N-Cyclohexyl-2-benzyloxy-1,3-dioxo-1,2,3,4-tetrahydroisoquinoline-4-carboxamide (15). White solid (85%); mp 192 °C; 100% keto form; 1H NMR (300 MHz, DMSO- d_6): $\delta = 1.15$ – 1.35 (m, 6 H, 3 CH_2), 1.47–1.86 (m, 4 H, 2 CH_2), 3.46 (m, 1 H, CH), 4.98 (d, 1 H, OCH_2 , $^2J = 9.6$ Hz), 5.03 (d, 1 H, OCH_2 , $^2J = 9.6$ Hz), 5.11 (s, 1 H, CH), 7.39–7.48 (m, 4 H, H_{Ar}), 7.52–7.62 (m, 3 H, H_{Ar}), 7.73 (td, 1 H, H_{Ar} , $^3J = 7.6$ Hz, $^4J = 1.3$ Hz), 8.09 (dd, 1 H, H_8 , $^3J = 7.8$ Hz, $^4J = 1.0$ Hz), 8.69 (d_{app} , 1 H, NH, $^3J = 7.7$ Hz); ^{13}C NMR (75 MHz, DMSO- d_6): $\delta = 24.2$ (CH_2), 25.1 (2 CH_2), 32.0 (2 CH_2), 48.2 (CH), 55.6 (CH), 77.7 (OCH_2), 125.3 (C_{IV}), 126.4 (CH), 128.0 (CH), 128.2 (CH), 128.4 (2 CH), 128.8 (CH), 129.4 (2 CH), 134.1 (CH), 134.5 (C_{IV}), 134.9 (C_{IV}), 161.0 (CO), 164.5 (CO), 165.0 (CO); ESI-MS: $m/z = 393$ (M + H) $^+$.

4.1.2.15. (2-Benzyloxy-1,3-dioxoisoquinolin-4-yl)(piperidin-1-yl)methanone (16). White solid (67%); mp 132 °C; 100% keto form; 1H NMR (300 MHz, DMSO- d_6): $\delta = 1.48$ – 1.62 (m, 6 H, 3 CH_2), 3.35 (t, 2 H, N- CH_2 , $^3J = 5.1$ Hz), 3.66 (t, 2 H, N- CH_2 , $^3J = 5.1$ Hz), 5.00 (s, 2 H, OCH_2), 5.93 (s, 1 H, CH), 7.30 (d, 1 H, H_{Ar} , $^3J = 7.2$ Hz), 7.42–7.56 (m, 6 H, H_{Ar}), 7.74 (t, 1 H, H_{Ar} , $^3J = 7.2$ Hz), 8.12 (d, 1 H, H_8 , $^3J = 7.7$ Hz); ^{13}C NMR (75 MHz, DMSO- d_6): $\delta = 23.8$ (CH_3), 25.3 (CH_2), 26.1 (CH_2), 43.2 (CH_2), 47.5 (CH_2), 51.0 (CH), 77.5 (OCH_2), 125.4 (C_{IV}), 126.9 (CH), 128.1 (CH), 128.3 (CH), 128.4 (2 CH), 128.9 (CH), 129.4 (2 CH), 134.2 (CH), 134.3 (C_{IV}), 135.1 (C_{IV}), 160.9 (CO), 164.4 (CO), 164.6 (CO); ESI-MS: $m/z = 379$ (M + H) $^+$.

4.1.3. Deprotection of the precursors 2–16

4.1.3.1. N-Propyl-2-hydroxy-1,3-dioxo-1,2,3,4-tetrahydroisoquinoline-4-carboxamide (17). Intermediate **2** (0.265 g, 0.74 mmol) was dissolved in a mixture of ethyle acetate (10 mL) and methanol (5 mL) and hydrogenated for 4 h at room temperature over Pd/C 5% (20 mg). The catalyst was filtered and the solvent was removed *in vacuo*. Trituration of the residue in ether afforded the deprotected compound **15** as a white solid (90%); mp 180 °C; 100% keto form; 1H NMR (300 MHz, DMSO- d_6): $\delta = 0.92$ (t, 3 H, CH_3 , $^3J = 7.1$ Hz), 1.51 (sext, 2 H, NH- CH_2 - CH_2 , $^3J = 7.0$ Hz), 3.11 (d_{app} , 2 H, NH- CH_2 , $^3J = 5.6$ Hz), 5.13 (s, 1 H, CH), 7.46 (d, 1 H, H_{Ar} , $^3J = 7.7$ Hz), 7.60 (t, 1 H, H_{Ar} , $^3J = 7.2$ Hz), 7.76 (t, 1 H, H_{Ar} , $^3J = 7.2$ Hz), 8.11 (d, 1 H, H_8 , $^3J = 7.7$ Hz), 8.82 (m, 1 H, NH), 10.80 (s, 1 H, OH); ^{13}C NMR (75 MHz, DMSO- d_6): $\delta = 11.3$ (CH_3), 22.1 (CH_2), 40.9 (CH_2), 55.4 (CH), 125.4 (C_{IV}), 126.6 (CH), 127.9 (CH), 133.8 (CH), 134.7 (C_{IV}), 161.6 (CO), 164.8 (CO), 166.1 (CO); ESI-MS: $m/z = 263$ (M + H) $^+$; HRMS calcd for $C_{13}H_{14}N_2O_4$ 262.09536; found: 262.09355; Anal. Calc. For $C_{13}H_{14}N_2O_4$: C, 59.54, H, 5.38, N, 10.68; Found: C, 59.67, H,

5.39, N, 10.66.

4.1.3.2. N-Isopropyl-2-hydroxy-1,3-dioxo-1,2,3,4-tetrahydroisoquinoline-4-carboxamide (18). Intermediate **3** (0.35 g, 1.0 mmol) was dissolved in a minimum of CH_2Cl_2 and boron trichloride (1.0 M solution in CH_2Cl_2 , 6.0 mL, 6.0 mmol) was added dropwise at room temperature. The solution was stirred for 15 min and water (20 mL) was slowly added. After 5 min stirring, the precipitate was filtered and the aqueous layer was extracted with ethyle acetate. Organic layers were dried over Na_2SO_4 and concentrated *in vacuo*. Organic residues and precipitate were gathered and triturated with ether. Insoluble materials were filtered and dried at room temperature giving compound **16** as a beige solid (56%); mp 190 °C; 100% keto form; 1H NMR (300 MHz, DMSO- d_6): $\delta = 1.12$ (d, 3 H, CH_3 , $^3J = 6.5$ Hz), 1.19 (d, 3 H, CH_3 , $^3J = 6.5$ Hz), 3.80 (sext, 1 H, CH, $^3J = 6.5$ Hz), 5.07 (s, 1 H, CH), 7.45 (d, 1 H, H_{Ar} , $^3J = 7.7$ Hz), 7.60 (t, 1 H, H_{Ar} , $^3J = 7.7$ Hz), 7.77 (t, 1 H, H_{Ar} , $^3J = 7.3$ Hz), 8.12 (d, 1 H, H_8 , $^3J = 7.5$ Hz), 8.75 (d_{app} , 1 H, NH, $^3J = 7.3$ Hz); ^{13}C NMR (75 MHz, DMSO- d_6): $\delta = 22.1$ (2 CH_3), 41.3 (CH), 55.3 (CH), 125.4 (C_{IV}), 126.4 (CH), 127.9 (CH), 128.2 (CH), 133.8 (CH), 134.7 (C_{IV}), 161.6 (CO), 164.8 (CO), 165.1 (CO); ESI-MS: $m/z = 263$ (M + H) $^+$; HRMS calcd for $C_{13}H_{14}N_2O_4$ 262.09536; found: 262.09605; Anal. Calc. For $C_{13}H_{14}N_2O_4$: C, 59.54, H, 5.38, N, 10.68; Found: C, 59.45, H, 5.37, N, 10.67.

4.1.3.3. N-Butyl-2-hydroxy-1,3-dioxo-1,2,3,4-tetrahydroisoquinoline-4-carboxamide (19). Hydrogenation over Pd/C 5%. White solid (53%); mp 180 °C; 100% keto form; 1H NMR (300 MHz, DMSO- d_6): $\delta = 0.92$ (t, 3 H, CH_3 , $^3J = 7.0$ Hz), 1.15–1.36 (m, 4 H, 2 CH_2), 3.25 (q, 2 H, NH- CH_2 , $^3J = 7.0$ Hz), 5.00 (s, 1 H, CH), 7.40 (d, 1 H, H_{Ar} , $^3J = 7.7$ Hz), 7.69 (t, 1 H, H_{Ar} , $^3J = 7.4$ Hz), 7.69 (t, 1 H, H_{Ar} , $^3J = 7.4$ Hz), 8.15 (d, 1 H, H_8 , $^3J = 8.1$ Hz), 8.72 (d_{app} , 1 H, NH, $^3J = 7.0$ Hz), 10.45 (s, 1 H, OH); ^{13}C NMR (75 MHz, DMSO- d_6): $\delta = 14.0$ (CH_3), 19.8 (CH_2), 31.3 (CH_2), 39.2 (CH_2), 55.8 (CH), 125.8 (C_{IV}), 127.0 (CH), 128.3 (CH), 128.6 (CH), 135.1 (C_{IV}), 162.0 (CO), 165.2 (CO), 166.4 (CO); ESI-MS: $m/z = 277$ (M + H) $^+$; HRMS calcd for $C_{14}H_{16}N_2O_4$ 276.11101; found: 276.11213; Anal. Calc. For $C_{14}H_{16}N_2O_4$: C, 60.86, H, 5.84, N, 10.14; Found: C, 60.98, H, 5.83, N, 10.11.

4.1.3.4. N-Butyl-N-methyl-2-hydroxy-1,3-dioxo-1,2,3,4-tetrahydroisoquinoline-4-carboxamide (20). Hydrogenation over Pd/C 5%. Brown solid (62%); mp 120–124 °C; 100% keto form; 1H NMR (300 MHz, DMSO- d_6): $\delta = 0.92$ (t, 3 H, CH_3 , $^3J = 8.4$ Hz), 1.27–1.70 (m, 4 H, 2 CH_2), 2.95 (s, 3 H, NH- CH_3), 3.34 (m, 2 H, NH- CH_2), 5.90 (s, 1 H, CH), 7.32 (d, 1 H, H_{Ar} , $^3J = 7.5$ Hz), 7.61 (t, 1 H, H_{Ar} , $^3J = 7.5$ Hz), 7.76 (d, 1 H, H_{Ar} , $^3J = 7.5$ Hz), 8.12 (d, 1 H, H_8 , $^3J = 7.2$ Hz); ^{13}C NMR (75 MHz, $CDCl_3$): $\delta = 14.2$ (CH_3), 19.8 (CH_2), 29.0 (CH_2), 31.0 (CH_2), 34.2 (NH CH_3), 36.7 (NH CH_3), 47.7 (NH CH_2), 50.7 (NH CH_2), 51.0 (CH), 51.5 (CH), 126.0 (C_{IV}), 127.3 (CH), 128.3 (CH), 128.6 (CH), 134.3 (CH), 135.6 (C_{IV}), 161.9 (CO), 165.2 (CO), 167.3 (CO); ESI-MS: $m/z = 291$ (M + H) $^+$; HRMS calcd for $C_{15}H_{18}N_2O_4$ 290.12666; found: 290.12567; Anal. Calc. For $C_{15}H_{18}N_2O_4$: C, 62.06, H, 6.25, N, 9.65; Found: C, 62.21, H, 6.23, N, 9.66.

4.1.3.5. N,N-Diethyl-2-hydroxy-1,3-dioxo-1,2,3,4-tetrahydroisoquinoline-4-carboxamide (21). Hydrogenation over Pd/C 5%. White solid (52%); mp 178 °C; 100% keto form; 1H NMR (300 MHz, DMSO- d_6): $\delta = 1.21$ (t, 3 H, CH_3 , $^3J = 6.4$ Hz), 1.28 (t, 3 H, CH_3 , $^3J = 6.6$ Hz), 3.21–3.41 (m, 2 H, NH- CH_2), 3.60–3.73 (m, 2 H, NH- CH_2), 5.77 (s, 1 H, CH), 7.22 (d, 1 H, H_{Ar} , $^3J = 7.7$ Hz), 7.55 (t, 1 H, H_{Ar} , $^3J = 7.6$ Hz), 7.70 (t, 1 H, H_{Ar} , $^3J = 7.5$ Hz), 8.08 (d, 1 H, H_8 , $^3J = 7.7$ Hz), 10.50 (s, 1 H, OH); ^{13}C NMR (75 MHz, DMSO- d_6): $\delta = 12.7$ (CH_3), 14.8 (CH_3), 40.4 (CH_2), 42.8 (CH_2), 50.6 (CH), 125.5 (C_{IV}), 126.5 (CH), 127.9 (CH), 128.0 (CH), 133.9 (CH), 135.3 (C_{IV}), 161.5 (CO), 164.8 (CO), 166.0 (CO); ESI-MS: $m/z = 277$ (M + H) $^+$; HRMS

calcd for C₁₄H₁₆N₂O₄ 276.11101; found: 276.11170; Anal. Calc. For C₁₄H₁₆N₂O₄: C, 60.86, H, 5.84, N, 10.14; Found: C, 60.69, H, 5.86, N, 10.11.

4.1.3.6. N-Tert-butyl-2-hydroxy-1,3-dioxo-1,2,3,4-tetrahydroisoquinoline-4-carboxamide (22). Treatment with boron trichloride. White solid (49%); mp 174 °C; 100% keto form; ¹H NMR (300 MHz, DMSO-*d*₆): δ = 1.25 (s, 9 H, 3 CH₃), 5.09 (s, 1 H, CH), 7.42 (d, 1 H, H_{Ar}, ³J = 7.3 Hz), 7.53 (t, 1 H, H_{Ar}, ³J = 7.7 Hz), 7.70 (t, 1 H, H_{Ar}, ³J = 7.7 Hz), 8.05 (d, 1 H, H₈, ³J = 7.7 Hz), 8.47 (s, 1 H, NH); ¹³C NMR (75 MHz, DMSO-*d*₆): δ = 28.1 (3 CH₃), 50.9 (C_{IV}), 55.7 (CH), 125.3 (C_{IV}), 126.3 (CH), 127.8 (CH), 128.0 (CH), 133.7 (CH), 134.9 (C_{IV}), 161.6 (CO), 164.9 (CO), 165.3 (CO); ESI-MS: *m/z* = 277 (M + H)⁺; HRMS calcd for C₁₄H₁₆N₂O₄ 276.11101; found: 276.10935; Anal. Calc. For C₁₄H₁₆N₂O₄: C, 60.86, H, 5.84, N, 10.14; Found: C, 61.05, H, 5.86, N, 10.15.

4.1.3.7. N-Pentyl-2-hydroxy-1,3-dioxo-1,2,3,4-tetrahydroisoquinoline-4-carboxamide (23). Hydrogenation over Pd/C 5%. White solid (52%); mp 130 °C (dec); 100% keto form; ¹H NMR (300 MHz, DMSO-*d*₆): δ = 0.80 (t, 3 H, CH₃, ³J = 6.6 Hz), 1.21–1.22 (m, 4 H, 2 CH₂), 1.37–1.39 (m, 2 H, CH₂), 3.00 (m, 2 H, NH–CH₂), 4.99 (s, 1 H, CH), 7.33 (d, 1 H, H_{Ar}, ³J = 7.0 Hz), 7.48 (t, 1 H, H_{Ar}, ³J = 7.0 Hz), 7.63 (t, 1 H, H_{Ar}, ³J = 7.0 Hz), 8.00 (d, 1 H, H₈, ³J = 7.5 Hz), 8.68 (m, 1 H, NH), 10.51 (s, 1 H, OH); ¹³C NMR (75 MHz, DMSO-*d*₆): δ = 14.3 (CH₃), 22.2 (CH₂), 28.9 (2 CH₂), 39.5 (CH₂), 55.8 (CH), 125.2 (C_{IV}), 127.0 (CH), 128.3 (CH), 128.6 (CH), 134.1 (CH), 135.3 (C_{IV}), 162.0 (CO), 165.2 (CO), 166.4 (CO); ESI-MS: *m/z* = 291 (M + H)⁺; HRMS calcd for C₁₅H₁₈N₂O₄ 290.12666; found: 290.12559; Anal. Calc. For C₁₅H₁₈N₂O₄: C, 62.06, H, 6.25, N, 9.65; Found: C, 62.15, H, 6.23, N, 9.68.

4.1.3.8. N-Hexyl-2-hydroxy-1,3-dioxo-1,2,3,4-tetrahydroisoquinoline-4-carboxamide (24). Treatment with boron trichloride. Light brown solid (79%); mp 137–138 °C; 90% keto form; 10% enol form; **Keto form**; ¹H NMR (300 MHz, DMSO-*d*₆): δ = 0.89 (t, 3 H, CH₃, ³J = 7.0 Hz), 1.24 (m, 6 H, CH₂), 1.40 (quin, 2 H, CH₂, ³J = 7.0 Hz), 3.05 (m, 2 H, CH₂), 5.05 (s, 1 H, CH), 7.38 (dd, 1 H, H₅, ³J = 8.0 Hz, ⁴J = 1.5 Hz), 7.54 (td, 1 H, H_{Ar}, ³J = 8.0 Hz, ⁴J = 1.5 Hz), 7.69 (td, 1 H, H_{Ar}, ³J = 8.0 Hz, ⁴J = 1.5 Hz), 8.05 (dd, 1 H, H₈, ³J = 8.0 Hz, ⁴J = 1.5 Hz), 8.75 (t, 1 H, NH, ³J = 6.5 Hz); ¹³C NMR (75 MHz, DMSO-*d*₆): δ = 13.9 (CH₃), 22.0 (CH₂), 25.8 (CH₂), 28.7 (CH₂), 30.8 (CH₂), 40.1 (CH₂), 55.3 (CH), 125.3 (C_{IV}), 126.4 (CH), 127.8 (CH), 128.1 (CH), 133.7 (CH), 134.6 (C_{IV}), 161.5 (CO), 164.7 (CO), 165.9 (CO); **Enol form**; only several peaks could be attributed on the ¹H NMR spectrum; ¹H NMR (300 MHz, DMSO-*d*₆): δ = 0.73 (t, 3 H, CH₃, ³J = 7.0 Hz), 3.24 (t, 2 H, CH₂, ³J = 7.0 Hz), 7.32 (td, 1 H, H_{Ar}, ³J = 7.5 Hz, ⁴J = 1.2 Hz), 8.15 (dd, 1 H, H₈, ³J = 8.0 Hz, ⁴J = 1.2 Hz); ESI-MS: *m/z* = 305 (M + H)⁺; HRMS calcd for C₁₆H₂₀N₂O₄ 304.14231; found: 304.14043; Anal. Calc. For C₁₆H₂₀N₂O₄: C, 63.14, H, 6.62, N, 9.20; Found: C, 63.25, H, 6.61, N, 9.17.

4.1.3.9. N-Heptyl-2-hydroxy-1,3-dioxo-1,2,3,4-tetrahydroisoquinoline-4-carboxamide (25). Hydrogenation over Pd/C 5%. Grey solid (74%); mp 120–130 °C; 100% keto form; ¹H NMR (300 MHz, DMSO-*d*₆): δ = 0.90 (t, 3 H, CH₃, ³J = 7.0 Hz), 1.23–1.25 (m, 8 H, 4 CH₂), 1.40–1.42 (m, 2 H, CH₂), 3.07 (q, 2 H, NH–CH₂, ³J = 7.1 Hz), 5.08 (s, 1 H, CH), 7.40 (d, 1 H, H_{Ar}, ³J = 7.2 Hz), 7.55 (t, 1 H, H_{Ar}, ³J = 7.5 Hz), 7.70 (t, 1 H, H_{Ar}, ³J = 7.5 Hz), 8.11 (d, 1 H, H₈, ³J = 7.5 Hz), 8.82 (s, 1 H, NH); ¹³C NMR (75 MHz, DMSO-*d*₆): δ = 13.9 (CH₃), 22.0 (CH₂), 26.1 (CH₂), 28.3 (CH₂), 28.8 (CH₂), 31.2 (CH₂), 38.7 (CH₂), 55.3 (CH), 125.3 (C_{IV}), 126.4 (CH), 127.8 (CH), 128.1 (CH), 133.6 (CH), 134.6 (C_{IV}), 161.5 (CO), 164.7 (CO), 165.9 (CO); ESI-MS: *m/z* = 319 (M + H)⁺; HRMS calcd for C₁₇H₂₂N₂O₄ 318.15796; found: 318.15884; Anal. Calc. For C₁₇H₂₂N₂O₄: C, 64.13, H, 6.97, N, 8.80;

Found: C, 63.99, H, 6.95, N, 8.82.

4.1.3.10. N-Octyl-2-hydroxy-1,3-dioxo-1,2,3,4-tetrahydroisoquinoline-4-carboxamide (26). Hydrogenation over Pd/C 5%. Beige solid (67%); mp 92–96 °C; 100% keto form; ¹H NMR (300 MHz, DMSO-*d*₆): δ = 0.92 (t, 3 H, CH₃, ³J = 7.3 Hz), 1.29–1.31 (m, 10 H, 5 CH₂), 1.47–1.49 (m, 2 H, CH₂), 5.11 (s, 1 H, CH), 7.44 (d, 1 H, H_{Ar}, ³J = 7.3 Hz), 7.60 (t, 1 H, H_{Ar}, ³J = 7.0 Hz), 7.75 (t, 1 H, H_{Ar}, ³J = 7.0 Hz), 8.11 (d, 1 H, H₈, ³J = 7.3 Hz), 8.80 (s, 1 H, NH), 10.63 (s, 1 H, OH); ¹³C NMR (75 MHz, DMSO-*d*₆): δ = 13.9 (CH₃), 22.0 (CH₂), 26.2 (CH₂), 28.6 (2 CH₂), 28.7 (CH₂), 31.1 (CH₂), 39.0 (CH₂), 55.3 (CH), 125.3 (C_{IV}), 126.5 (CH), 127.8 (CH), 128.1 (CH), 133.6 (CH), 134.6 (C_{IV}), 161.5 (CO), 164.7 (CO), 165.9 (CO); ESI-MS: *m/z* = 333 (M + H)⁺; HRMS calcd for C₁₈H₂₄N₂O₄ 332.17361; found: 332.17889; Anal. Calc. For C₁₈H₂₄N₂O₄: C, 65.04, H, 7.28, N, 8.43; Found: C, 65.14, H, 7.27, N, 8.42.

4.1.3.11. N-Nonyl-2-hydroxy-1,3-dioxo-1,2,3,4-tetrahydroisoquinoline-4-carboxamide (27). Hydrogenation over Pd/C 5%. White solid (54%); mp 164 °C; 100% keto form; ¹H NMR (300 MHz, DMSO-*d*₆): δ = 0.70 (t, 3 H, CH₃, ³J = 7.0 Hz), 1.10–1.40 (m, 14 H, 7 CH₂), 3.05 (m, 2 H, NH–CH₂), 5.00 (s, 1 H, CH), 7.35 (d, 1 H, H_{Ar}, ³J = 7.0 Hz), 7.42 (t, 1 H, H_{Ar}, ³J = 7.0 Hz), 7.59 (t, 1 H, H_{Ar}, ³J = 7.0 Hz), 8.04 (d, 1 H, H₈, ³J = 7.5 Hz), 8.72 (m, 1 H, NH), 10.56 (s, 1 H, OH); ¹³C NMR (75 MHz, DMSO-*d*₆): δ = 13.9 (CH₃), 22.0 (CH₂), 26.2 (CH₂), 28.6 (CH₂), 28.7 (CH₂), 28.9 (CH₂), 29.5 (CH₂), 31.2 (CH₂), 39.0 (CH₂), 55.3 (CH), 125.3 (C_{IV}), 126.5 (CH), 127.8 (CH), 128.1 (CH), 133.6 (CH), 134.6 (C_{IV}), 161.5 (CO), 164.7 (CO), 165.9 (CO); ESI-MS: *m/z* = 347 (M + H)⁺; HRMS calcd for C₁₉H₂₆N₂O₄ 346.18926; found: 346.18787; Anal. Calc. For C₁₉H₂₆N₂O₄: C, 65.88, H, 7.57, N, 8.09; Found: C, 65.80, H, 7.55, N, 8.10.

4.1.3.12. N-Cyclopropyl-2-hydroxy-1,3-dioxo-1,2,3,4-tetrahydroisoquinoline-4-carboxamide (28). Treatment with boron trichloride. Brown solid (68%); mp 185–190 °C; 100% keto form; ¹H NMR (300 MHz, DMSO-*d*₆): δ = 0.38–0.52 (m, 2 H, 2 CH), 0.61–0.74 (m, 2 H, 2 CH), 2.64 (m, 1 H, CH), 4.96 (s, 1 H, CH), 7.35 (d, 1 H, H_{Ar}, ³J = 7.4 Hz), 7.55 (t, 1 H, H_{Ar}, ³J = 7.3 Hz), 7.70 (t, 1 H, H_{Ar}, ³J = 7.3 Hz), 8.10 (d, 1 H, H₈, ³J = 7.6 Hz), 8.87 (m, 1 H, NH); ¹³C NMR (75 MHz, DMSO-*d*₆): δ = 6.3 (CH₂), 22.9 (CH), 55.1 (CH), 125.5 (C_{IV}), 126.5 (CH), 127.9 (CH), 128.2 (CH), 133.8 (CH), 161.6 (CO), 165.0 (CO), 167.1 (CO); ESI-MS: *m/z* = 261 (M + H)⁺; HRMS calcd for C₁₃H₁₂N₂O₄ 260.07971; found: 260.07992; Anal. Calc. For C₁₃H₁₂N₂O₄: C, 60.00, H, 4.65, N, 10.76; Found: C, 59.91, H, 4.60, N, 10.74.

4.1.3.13. N-Cyclopentyl-2-hydroxy-1,3-dioxo-1,2,3,4-tetrahydroisoquinoline-4-carboxamide (29). Hydrogenation over Pd/C 5%. Brown solid (61%); mp 160 °C; 100% keto form; ¹H NMR (300 MHz, DMSO-*d*₆): δ = 1.40–1.80 (m, 8 H, 4 CH₂), 3.97 (m, 1 H, CH), 5.09 (s, 1 H, CH), 7.42 (d, 1 H, H_{Ar}, ³J = 7.0 Hz), 7.57 (t, 1 H, H_{Ar}, ³J = 7.2 Hz), 7.72 (t, 1 H, H_{Ar}, ³J = 7.3 Hz), 8.10 (d, 1 H, H₈, ³J = 7.6 Hz), 8.81 (d_{app}, 1 H, NH, ³J = 6.1 Hz), 10.63 (s, 1 H, OH); ¹³C NMR (75 MHz, DMSO-*d*₆): δ = 23.41 (CH₂), 23.45 (CH₂), 32.1 (CH₂), 32.2 (CH₂), 50.9 (CH), 55.1 (CH), 125.3 (C_{IV}), 126.3 (CH), 127.8 (CH), 128.1 (CH), 133.7 (CH), 134.7 (C_{IV}), 161.5 (CO), 164.7 (CO), 165.4 (CO); ESI-MS: *m/z* = 289 (M + H)⁺; HRMS calcd for C₁₅H₁₆N₂O₄ 288.11101; found: 288.11012; Anal. Calc. For C₁₅H₁₆N₂O₄: C, 62.49, H, 5.59, N, 9.72; Found: C, 62.56, H, 5.58, N, 9.70.

4.1.3.14. N-Cyclohexyl-2-hydroxy-1,3-dioxo-1,2,3,4-tetrahydroisoquinoline-4-carboxamide (30). Treatment with boron trichloride. Grey solid (76%); mp 165–170 °C; 100% keto form; ¹H NMR (300 MHz, DMSO-*d*₆): δ = 1.14–1.42 (m, 6 H, 3 CH₂), 1.46–1.94 (m, 4 H, 2 CH₂), 3.81 (m, 1 H, CH), 5.07 (s, 1 H, CH), 7.42 (d, 1 H, H_{Ar}, ³J = 7.6 Hz), 7.50 (t, 1 H, H_{Ar}, ³J = 7.4 Hz), 7.68 (t, 1 H, H_{Ar}, ³J = 7.0 Hz),

8.06 (d, 1 H, H₈, $^3J = 7.6$ Hz), 8.67 (d_{app}, 1 H, NH, $^3J = 7.2$ Hz), 10.57 (s, 1 H, OH); ^{13}C NMR (75 MHz, DMSO-*d*₆): $\delta = 24.3$ (2 CH₂), 25.3 (CH₂), 32.5 (2 CH₂), 47.1 (CH), 55.2 (CH), 120.4 (C_{IV}), 122.1 (CH), 124.2 (CH), 126.0 (CH), 130.8 (CH), 135.3 (C_{IV}), 158.9 (CO), 161.6 (CO), 164.8 (CO); ESI-MS: $m/z = 303$ (M + H)⁺; HRMS calcd for C₁₆H₁₈N₂O₄ 302.12666; found: 302.12654; Anal. Calc. For C₁₆H₁₈N₂O₄: C, 63.56, H, 6.00, N, 9.27; Found: C, 63.60, H, 6.02, N, 9.25.

4.1.3.15. (2-Hydroxy-1,3-dioxisoquinolin-4-yl)(piperidin-1-yl)methanone (31). Hydrogenation over Pd/C 5%. Black solid (64%); mp > 128 °C (dec); 100% keto form; ^1H NMR (300 MHz, DMSO-*d*₆): $\delta = 1.49$ – 1.64 (m, 6 H, 3 CH₂), 3.35 (t, 2 H, N-CH₂, $^3J = 5.1$ Hz), 3.66 (t, 2 H, N-CH₂, $^3J = 5.1$ Hz), 5.97 (s, 1 H, CH), 7.30 (d, 1 H, H_{Ar}, $^3J = 7.7$ Hz), 7.61 (t, 1 H, H_{Ar}, $^3J = 7.7$ Hz), 7.76 (t, 1 H, H_{Ar}, $^3J = 7.7$ Hz), 8.12 (d, 1 H, H₈, $^3J = 7.7$ Hz), 10.8 (s, 1 H, OH); ^{13}C NMR (75 MHz, DMSO-*d*₆): $\delta = 23.7$ (CH₃), 25.1 (CH₂), 26.0 (CH₂), 43.0 (CH₂), 47.4 (CH₂), 50.3 (CH), 125.3 (C_{IV}), 126.7 (CH), 127.7 (CH), 127.9 (CH), 133.7 (CH), 135.0 (C_{IV}), 161.3 (CO), 164.6 (CO), 164.7 (CO); ESI-MS: $m/z = 289$ (M + H)⁺; HRMS calcd for C₁₅H₁₆N₂O₄ 288.11101; found: 288.10986; Anal. Calc. For C₁₅H₁₆N₂O₄: C, 62.49, H, 5.59, N, 9.72; Found: C, 62.47, H, 5.60, N, 9.73.

4.2. Biological assays

4.2.1. Integrase inhibition

To determine the susceptibility of the HIV-1 integrase enzyme to different compounds, an enzyme-linked immunosorbent assay was used. This assay uses an oligonucleotide substrate in which one oligo (5'-ACTGCTAGAGATTTCCACTGACTAAAAGGGTC-3') is labeled with biotin on the 3' end and in which the other oligo is labeled with digoxigenin at the 5' end. For the overall integration assay, the second 5'-digoxigenin-labeled oligo is 5'-GACCCTTTAGTCAGTGTGGAAAATCTCTAGCACT-3'. For the strand transfer assay, a pre-cleaved oligonucleotide substrate (the second oligonucleotide lacks GT [underlined] at the 3' end) was used. The integrase was diluted in 750 mM NaCl, 10 mM Tris (pH 7.6), 10% glycerol, 1 mM β -mercaptoethanol, and 0.1 mg/mL bovine serum albumin. To perform the reaction, 4 μL of diluted integrase (corresponds to a concentration of WT integrase of 1.6 μM) and 4 μL of annealed oligos (7 nM) were added in a final reaction volume of 40 μL containing 10 mM MgCl₂, 5 mM dithiothreitol, 20 mM HEPES (pH 7.5), 0.5% polyethylene glycol, and 15% DMSO. As such, the final concentration of integrase in this assay was 160 nM. The reaction was carried out for 1 h at 37 °C. The reaction products were denatured with 30 mM NaOH and detected by ELISA on avidin-coated plates.

4.2.2. Time of addition experiments

100,000 MT-4 cells per well in a 96-well microtiter plate were infected with HIV-IIIB at a multiplicity of infection of 0.7. Compounds were added at different time points after infection (1, 2, 3, 4, 5, 6, 7, 8, 9, 10, 11, 12, 24 and 25h) as described previously [31]. Viral p24 antigen production was determined 30 h postinfection by ELISA (Innogenetics, Belgium). Compounds were added at 50 and 100 times their EC₅₀ as determined by the drug susceptibility assay (MTT/MT-4).

4.2.3. In vitro anti-HIV and drug susceptibility assays

The inhibitory effect of antiviral drugs on the HIV-1-induced cytopathic effect (CPE) in human lymphocyte MT-4 cell culture was determined by the MT-4/MTT assay. MT-4 cells were obtained through the AIDS Research and Reference Reagent Program, Division of AIDS, NIH. The cells were grown in RPMI 1640 supplemented with 10% FCS and 20 $\mu\text{g}/\text{mL}$ gentamicin (RPMI-complete). This assay is based on the reduction of the yellow colored 3-(4,5-

dimethylthiazol-2-yl)-2,5-diphenyltetrazolium bromide (MTT) by mitochondrial dehydrogenase of metabolically active cells to a blue formazan derivative, which can be measured spectrophotometrically. The 50% cell culture infective dose (CCID₅₀) of the HIV-1 (IIIB) strain was determined by titration of the virus stock using MT-4 cells. The origin of HIV-1 strain III_B has been described previously [32]. For the drug susceptibility assays, MT-4 cells were infected with 100–300 CCID₅₀ of the virus stock in the presence of 5-fold serial dilutions of the antiviral drugs. The concentration of various compounds achieving 50% protection against the CPE of the different HIV strains, which is defined as the EC₅₀, was determined. In parallel, the 50% cytotoxic concentration (CC₅₀) was determined.

4.2.4. Reverse transcriptase RNase H assay

The substrate for RNase H activity was prepared as previously described [33]. *E. coli* RNA polymerase used single-stranded calf thymus DNA as a template to synthesize complementary ³H-labeled RNA. For RNase H activity, recombinant HIV-1 RT (4.5 pmol) [34] was incubated with the appropriate compound for 10 min at 37 °C in 20 μL . The components of the incubation mixture were added to reach a final concentration of 50 mM Tris-HCl (pH 8.0), 10 mM dithiothreitol, 6 mM MgCl₂, 80 mM KCl, and the labeled nucleic acid duplex (20,000 cpm) in a final volume of 50 μL . After incubation for 10 min at 37 °C, the reaction was stopped by addition of 1 mL of cold 10% TCA containing 0.1 M sodium pyrophosphate, the acid-precipitable material was collected on nitrocellulose filters and washed, the radioactivity was determined and the radioactivity released from the hybrid was determined by subtraction from the undigested hybrid control.

4.2.5. ADMETox studies

Aqueous solubility (PBS, pH 7.4; Cerep catalogue reference 0435), partition coefficient (log D, *n*-octanol/PBS, pH 7.4; Cerep catalogue reference 0417), human plasma protein binding (Cerep catalogue reference 2194), A-B permeability coefficient (P_{app} , Caco-2 cells, pH 6.5/7.4; Cerep catalogue reference 3318), inhibition of P-gp efflux (MDR1-MDCKII, calcein AM substrate; Cerep catalogue reference 1324), inhibition of CYP1A2 (recombinant, CEC substrate, Cerep catalogue reference 0389), inhibition of CYP2C9 (recombinant, MFC substrate, Cerep catalogue reference 0412), inhibition of CYP2C19 (recombinant, CEC substrate, Cerep catalogue reference 0390), inhibition of CYP2D6 (recombinant, MFC substrate, Cerep catalogue reference 1338), inhibition of CYP3A4 (recombinant, BFC substrate, Cerep catalogue reference 0391), cardiac toxicity (hERG, automated patch clamp, Cerep catalogue reference 2245), *in vitro* cytotoxicity panel (cell number, intracellular free calcium, nuclear size, membrane permeability, mitochondrial membrane potential, <http://www.cerep.fr/cerep/users/pages/downloads/Documents/Marketing/Pharmacology%20&%20ADME/OTP/CytotoxicityPanel.pdf>) were determined in standard assays by Cerep, France (www.cerep.fr).

4.3. Docking procedure

We previously reported that the 2-hydroxyisoquinoline-1,3-(2H,4H)-dione scaffold complexes magnesium as the enol or enolate form, as shown by NMR studies [25]. Predictions of the ionization state by use of the SPARC online calculator [35] indicate that such enols are deprotonated in aqueous media at physiological pH in the presence of magnesium cations; hence ligands were modeled as the dianionic enolate form. Compounds **17**, **19**, **23**–**27** were thus created and their geometry minimized at the HF/3-21G level by use of the Gaussian 09 package [36]. The minimized ligands were then submitted to our previously reported docking protocol using the PDB 3S3M crystallographic structure, which was validated for this

pharmacophore. The co-crystallized ligand was extracted and the protein was prepared by adding hydrogens to the X-ray structure. Water molecules and irrelevant heteroatoms were removed. Magnesium cations were set to allow octahedral geometry. Docking calculations were carried out with the CCDC GOLD 5.2 docking suite [37]. The active site was defined as a sphere containing all atoms within 15 Å of the X-ray ligand centroid. A dynamic distance constraint d was introduced between O11 and H27 of the mol2 ligand structure ($1.0 \text{ \AA} < d < 2.4 \text{ \AA}$), and a library of 34 rotamers was enabled for Arg329. The CHEMPLP fitness function was used with modified parameters [38]. After manual editing of atom and bond types in mol2 files, both ligands were submitted to 400 docking runs with 0.75 Å RMSD clustering. The resulting docking poses were analyzed and selected poses were rendered with the UCSF Chimera software [39].

Acknowledgments

This work was financially supported by grants from la région Nord Pas-de-Calais and le Centre National de la Recherche Scientifique (CNRS) (Muriel Billamboz's PhD), le Ministère de l'Enseignement Supérieur et de la Recherche Française (Virginie Suchaud's PhD) and fundings from l'Agence Nationale de la Recherche contre le Sida (ANRS; october 2014–december 2015, first call for bids 2014, decision 14394; october 2011–october 2013, second call for bids 2011, decision 11349; march 2005–february 2007, first call for bids 2005, decision 2005/003). Experiments at KU Leuven were funded by the FP7 project CHAARM and the IWT.

Appendix A. Supplementary data

Supplementary data related to this article can be found at <http://dx.doi.org/10.1016/j.ejmech.2016.03.083>.

References

- [1] R.V. Patel, Y.S. Keum, S.W. Park, Sketching the historical development of pyrimidines as the inhibitors of the HIV integrase, *Eur. J. Med. Chem.* 97 (2015) 649–653.
- [2] V. Summa, A. Petrocchi, F. Bonelli, B. Crescenzi, M. Donghi, M. Ferrara, F. Fiore, C. Gardelli, O.G. Paz, D.J. Hazuda, P. Jones, O. Kinzel, R. Laufer, E. Monteagudo, E. Muraglia, E. Nizi, F. Orvieto, P. Pace, G. Pescatore, R. Scarpelli, K. Stillmock, M.V. Witmer, M. Rowley, Discovery of raltegravir, a potent, selective orally bioavailable HIV-integrase inhibitor for the treatment of HIV-AIDS infection, *J. Med. Chem.* 51 (2008) 5843–5855.
- [3] D.J. McColl, X. Chen, Strand transfer inhibitors of HIV-1 integrase: bringing IN a new era of antiretroviral therapy, *Antivir. Res.* 85 (2010) 101–118.
- [4] J.J. Eron, D.A. Cooper, R.T. Steigbigel, B. Clotet, J.M. Gatell, P.N. Kumar, J.K. Rockstroh, M. Schechter, M. Markowitz, P. Yeni, M.R. Loufy, A. Lazzarin, J.L. Lennox, K.M. Strohmaier, H. Wan, R.J. Barnard, B.Y. Nguyen, H. Tepler, Efficacy and safety of raltegravir for treatment of HIV for 5 years in the BENCHMRK studies: final results of two randomized, placebo-controlled trials, *Lancet Infect. Dis.* 13 (2013) 587–596.
- [5] M.A. Thompson, J.A. Aberg, P. Cahn, J.S. Montaner, G. Rizzardini, A. Telenti, J.M. Gatell, H.F. Gunthard, S.M. Hammer, M.S. Hirsch, D.M. Jacobsen, P. Reiss, D.D. Richman, P.A. Volberding, P. Yeni, R.T. Schooley, Antiretroviral treatment of adult HIV infection: 2010 recommendations of the international AIDS society-USA panel, *JAMA, J. Am. Med. Assoc.* 304 (2010) 321–333.
- [6] M. Metifiot, C. Marchand, K. Maddali, Y. Pommier, Resistance to integrase inhibitors, *Viruses* 2 (2010) 1347–1366.
- [7] S. Fransen, S. Gupta, R. Danovich, D. Hazuda, M. Miller, M. Witmer, C.J. Petropoulos, W. Huang, Loss of raltegravir susceptibility by human immunodeficiency virus type 1 is conferred via multiple nonoverlapping genetic pathways, *J. Virol.* 83 (2009) 11440–11446.
- [8] L. Menendez-Arias, Molecular basis of human immunodeficiency virus type 1 drug resistance: overview and recent developments, *Antivir. Res.* 98 (2013) 93–120.
- [9] M.A. Wainberg, G.J. Zaharatos, B.G. Brenner, Development of antiretroviral drug resistance, *N. Engl. J. Med.* 365 (2011) 637–646.
- [10] P.E. Sax, E. De Jesus, A. Mills, A. Zolopa, C. Cohen, D. Wohl, J.E. Gallant, H.C. Liu, L. Zhong, K. Yale, et al., Co-formulated elvitegravir, cobicistat, emtricitabine, and tenofovir versus co-formulated efavirenz, emtricitabine, and tenofovir for initial treatment of HIV-1 infection: a randomized, double-blinded, phase 3 trial, analysis of results after 48 weeks, *Lancet* 379 (2012) 2439–2448.
- [11] J.M. Molina, A. Lamarca, J. Andrade-Villanueva, B. Clotet, N. Clumeck, Y.P. Liu, L. Zhong, N. Margot, A.K. Cheng, S.L. Chuck, Efficacy and safety of once daily elvitegravir versus twice daily raltegravir in treatment-experienced patients with HIV-1 receiving a ritonavir-boosted protease inhibitor: randomized, double-blind, phase 3, non-inferiority study, *Lancet Infect. Dis.* 12 (2012) 27–35.
- [12] C. Marchand, The elvitegravir quad pill: the first once-daily dual-target anti-HIV tablet, *Expert. Opin. Investig. Drugs.* 21 (2012) 901–904.
- [13] R. Schrijvers, Z. Debyser, Combinational therapies for HIV: a focus on EVG/COBI/FTC/TDF, *Expert. Opin. Pharmacother.* 13 (2012) 1969–1983.
- [14] K. Shimura, E. Kodama, Y. Sakagami, Y. Matsuzaki, W. Watanabe, K. Yamataka, Y. Watanabe, Y. Ohata, S. Doi, M. Sato, M. Kano, S. Ikeda, M. Matsuoka, Broad antiretroviral activity and resistance profile of the novel human immunodeficiency virus integrase inhibitor Elvitegravir (JTK-303/GS-9137), *J. Virol.* 82 (2008) 764–774.
- [15] A.D. Ballantyne, C.M. Perry, Dolutegravir: first global approval, *Drugs* 73 (2013) 1627–1637.
- [16] F. Bailly, P. Cotelte, The preclinical discovery and development of dolutegravir for the treatment of HIV, *Expert. Opin. Drug Discov.* 10 (2015) 1243–1253.
- [17] M. Cruciani, M. Malena, Combination dolutegravir-abacavir-lamivudine in the management of HIV/AIDS: clinical utility and patient considerations, *Patient Prefer. Adherence* 9 (2015) 299–310.
- [18] P.K. Quashie, T. Mespelde, M.A. Wainberg, Evolution of HIV integrase resistance mutations, *Curr. Opin. Infect. Dis.* 26 (2013) 43–49.
- [19] L. Menéndez-Arias, M. Alvarez, Antiretroviral therapy and drug resistance in human immunodeficiency virus type 2 infection, *Antivir. Res.* 102 (2014) 70–86.
- [20] S. Hare, S.S. Gupta, E. Valkov, A. Engelman, P. Cherepanov, Retroviral intasome assembly and inhibition of DNA strand transfer, *Nature* 464 (2010) 232–236.
- [21] S. Hare, S.J. Smith, M. Métiéfiot, A. Jaxa-Chamier, Y. Pommier, S.H. Hughes, P. Cherepanov, Structural and functional analyses of the second-generation integrase strand transfer inhibitor Dolutegravir (S/GSK1349572), *Mol. Pharmacol.* 80 (2011) 565–572.
- [22] G. Cuzzucoli Crucitti, L. Pescatori, A. Messori, V.N. Madia, G. Pupo, F. Saccoliti, L. Scipione, S. Tortorella, F.S. Di Leva, S. Cosconati, E. Novellino, Z. Debyser, F. Christ, R. Costi, R. Di Santo, Discovery of N-aryl-naphthylamines as *in vitro* inhibitors of the interaction between HIV integrase and the cofactor LEDGF/p75, *Eur. J. Med. Chem.* 101 (2015) 288–294.
- [23] F. Christ, Z. Debyser, HIV-1 integrase inhibition: looking at cofactor interactions, *Future Med. Chem.* 7 (2015) 2407–2410.
- [24] X.Z. Zhao, S.J. Smith, D.P. Maskell, M. Metifiot, V.E. Pye, K. Fesen, C. Marchand, Y. Pommier, P. Cherepanov, S.H. Hughes, T.R. Burke Jr., HIV-1 Integrase strand transfer inhibitors with reduced susceptibility to drug resistant mutant integrases, *ACS Chem. Biol.* (2016), <http://dx.doi.org/10.1021/acscmbio.5b00948>.
- [25] M. Billamboz, F. Bailly, M.L. Barreca, L. De Luca, J.F. Mouscadet, C. Calmels, M.L. Andreola, F. Christ, Z. Debyser, M. Witvrouw, P. Cotelte, Design, synthesis and biological evaluation of a series of 2-hydroxyisoquinoline-1,3(2H,4H)-diones as dual inhibitors of human immunodeficiency virus type 1 integrase and reverse transcriptase RNase H domain, *J. Med. Chem.* 51 (2008) 7717–7730.
- [26] M. Billamboz, F. Bailly, C. Lion, C. Calmels, M.L. Andreola, M. Witvrouw, F. Christ, Z. Debyser, L. De Luca, A. Chimirri, P. Cotelte, 2-Hydroxyisoquinoline-1,3(2H,4H)-diones as inhibitors of HIV-1 integrase and reverse transcriptase RNase H domain: influence of the alkylation of position 4, *Eur. J. Med. Chem.* 46 (2011) 535–546.
- [27] B.A. Desimie, J. Demeulemeester, V. Suchaud, O. Taltynov, M. Billamboz, C. Lion, F. Bailly, S.V. Strelkov, Z. Debyser, P. Cotelte, F. Christ, 2-Hydroxyisoquinoline-1,3(2H,4H)-diones (HIDs), novel inhibitors of HIV integrase with a high barrier to resistance, *ACS Chem. Biol.* 8 (2013) 1187–1194.
- [28] M. Billamboz, V. Suchaud, F. Bailly, C. Lion, F. Christ, Z. Debyser, P. Cotelte, 4-Substituted 2-hydroxyisoquinoline-1,3-(2H-4H)-diones as a novel class of HIV-1 integrase inhibitors, *ACS Med. Chem. Lett.* 4 (2013) 606–611.
- [29] V. Suchaud, F. Bailly, C. Lion, C. Calmels, M.L. Andreola, F. Christ, Z. Debyser, P. Cotelte, Investigation of a novel series of 2-hydroxyisoquinoline-1,3(2H,4H)-diones (HIDs) as human immunodeficiency virus type 1 integrase inhibitors, *J. Med. Chem.* 57 (2014) 4640–4660.
- [30] C.R. Martinez, B.L. Iverson, Rethinking the term “pi-stacking”, *Chem. Sci.* 3 (2012) 2191–2201.
- [31] R. Pauwels, K. Andries, J. Desmyter, D. Schols, M.J. Kulda, H.J. Breslin, A. Raeymaeckers, J. Van Gelder, R. Woestenborghs, J. Heykants, Potent and selective inhibition of HIV-1 replication *in vitro* by a novel series of TIBO derivatives, *Nature* 343 (1990) 470–474.
- [32] A. Adachi, H.E. Gendelman, S. Koenig, T. Folks, R. Willey, A. Rabson, M.A. Martin, Production of acquired immunodeficiency syndrome-associated retrovirus in human and nonhuman cells transfected with an infectious molecular clone, *J. Virol.* 59 (1986) 284–291.
- [33] K. Moelling, T. Schulze, H. Diringier, Inhibition of human immunodeficiency virus type 1 RNase H by sulfated polyanions, *J. Virol.* 63 (1989) 5489–5491.
- [34] E. Dufour, J. Reinbolt, M. Castroviejo, B. Ehresmann, S. Litvak, L. Tarrago-Litvak, M.L. Andreola, Cross-linking localization of a HIV-1 reverse transcriptase peptide involved in the binding of primer tRNA_{Lys3}, *J. Mol. Biol.* 285 (1999) 1339–1346.
- [35] S.H. Hilal, S.W. Karickhoff, L.A. Carreira, A rigorous test for SPARC's chemical reactivity models: estimation of more than 4300 ionization pK_as, *Quant.*

- Struct.-Act. Relat. 14 (1995) 348–355.
- [36] M.J. Frisch, G.W. Trucks, H.B. Schlegel, G.E. Scuseria, M.A. Robb, J.R. Cheeseman, G. Scalmani, V. Barone, B. Mennucci, G.A. Petersson, H. Nakatsuji, M. Caricato, X. Li, H.P. Hratchian, A.F. Izmaylov, J. Bloino, G. Zheng, J.M. Sonnenberg, M. Ehara, K. Toyota, R. Fukuda, J. Hasegawa, M. Ishida, T. Nakajima, Y. Honda, O. Kitao, H. Nakai, T. Vreven, J.A. Montgomery Jr., J.E. Peralta, F. Ogliaro, M. Bearpark, J.J. Heyd, E. Brothers, K.N. Kudin, V.N. Staroverov, R. Kobayashi, J. Normand, K. Raghavachari, A. Rendell, J.C. Burant, S.S. Iyengar, J. Tomasi, M. Cossi, N. Rega, N.J. Millam, M. Klene, J.E. Knox, J.B. Cross, V. Bakken, C. Adamo, J. Jaramillo, R. Gomperts, R.E. Stratmann, O. Yazyev, A.J. Austin, R. Cammi, C. Pomelli, J.W. Ochterski, R.L. Martin, K. Morokuma, V.G. Zakrzewski, G.A. Voth, P. Salvador, J.J. Dannenberg, S. Dapprich, A.D. Daniels, Ö. Farkas, J.B. Foresman, J.V. Ortiz, J. Cioslowski, D.J. Fox, Gaussian 09, Revision D.01, Gaussian Inc., Wallingford, CT, 2009.
- [37] (a) G. Jones, P. Willett, R.C. Glen, A.R. Leach, R. Taylor, Development and validation of a genetic algorithm for flexible docking, *J. Mol. Biol.* 267 (1997) 727–748; (b) J.C. Cole, J.W.M. Nissink, R. Taylor, in: B. Shoichet, J. Alvarez (Eds.), *Virtual Screening in Drug Discovery*, CRC Press, Taylor & Francis Group, Boca Raton, FL, 2005.
- [38] O. Korb, T. Stützel, T. Exner, Empirical scoring functions for advanced protein-ligand docking with PLANTS, *J. Chem. Inf. Model.* 49 (2009) 84–96.
- [39] E.F. Pettersen, T.D. Goddard, C.C. Huang, G.S. Couch, D.M. Greenblatt, E.C. Meng, T.E.U.C.S.F. Ferrin, Chimera—a visualization system for exploratory research and analysis, *J. Comput. Chem.* 25 (2004) 1605–1612.